Structural behaviour of masonry arches on moving supports: from on-site observation to experimental and numerical analysis

2023 TMS Annual Meeting
Albuquerque, New Mexico
November 9, 2023

Chiara Ferrero
Postdoctoral fellow
University of Genoa, Italy

OUTLINE

- Background and motivation
- Objectives and methodology
- Results
  - Experimental tests
  - Numerical simulations
- Conclusions
- Future work

BACKGROUND AND MOTIVATION

- Nowadays, we have effective tools to assess the performance of large complex three-dimensional structures under a variety of natural and anthropic hazards.

BACKGROUND AND MOTIVATION

- Nowadays, we have effective tools to assess the performance of large complex three-dimensional structures under a variety of natural and anthropic hazards.

- **Why should we (still) study the response of masonry arches to support displacements?**

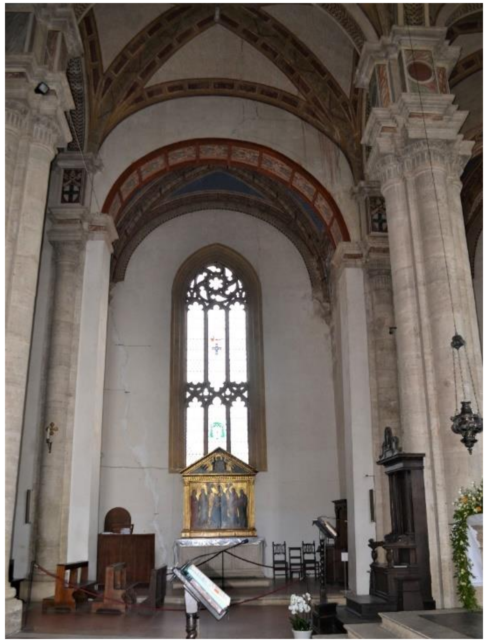

BACKGROUND AND MOTIVATION

- Masonry arches are widespread in cultural heritage buildings and play a primary role in their structural response.

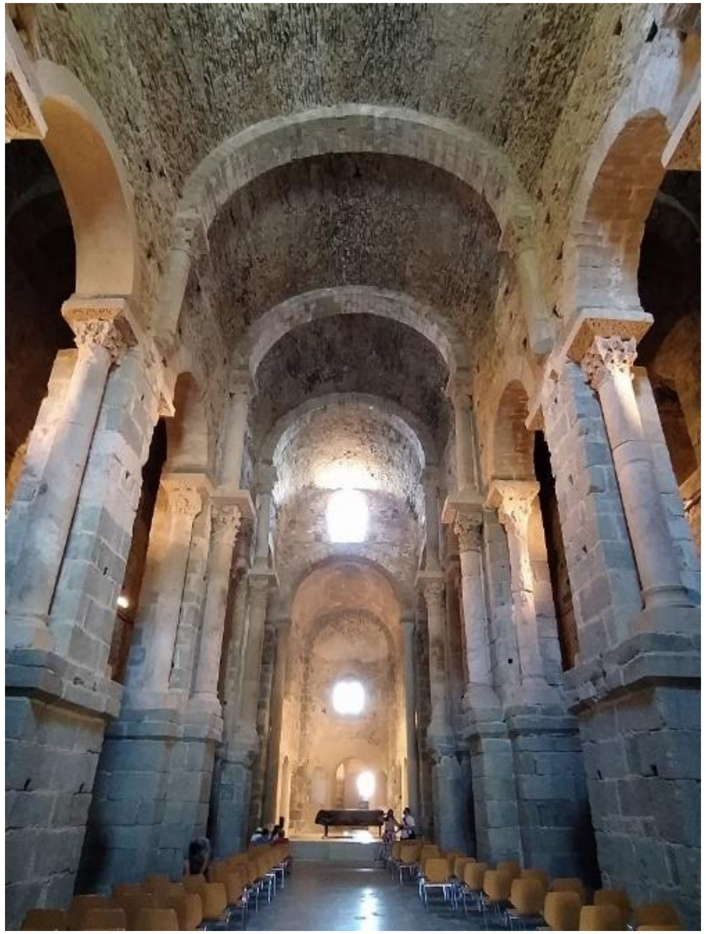

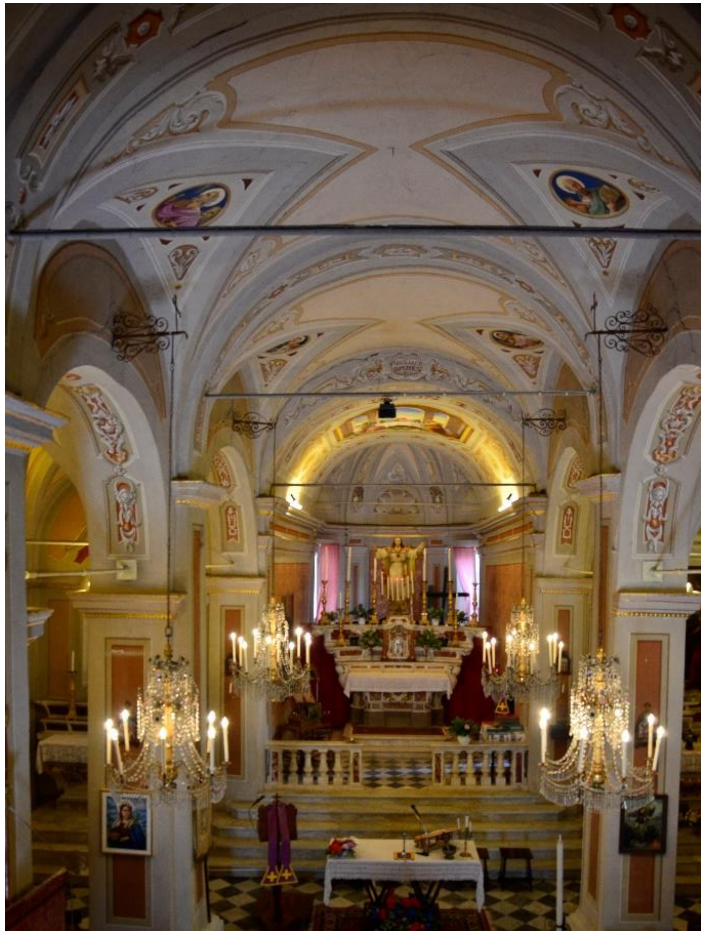

BACKGROUND AND MOTIVATION

- Large support displacements are a major threat to the stability of arches and may cause severe damage and large deformations.





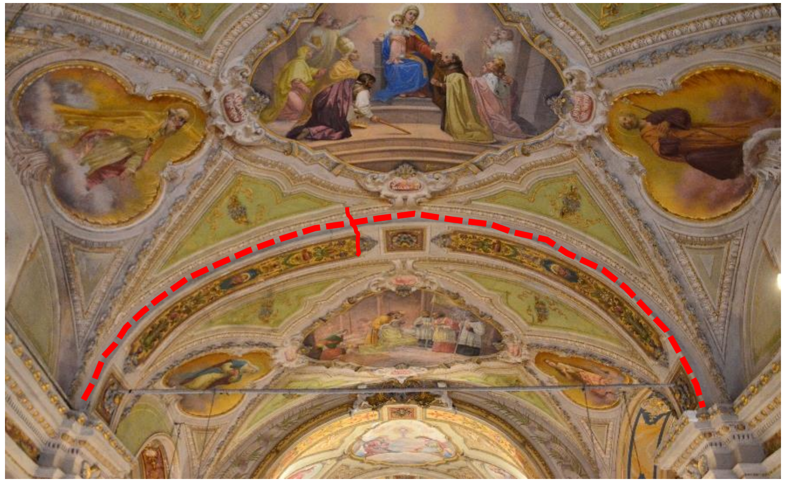

BACKGROUND AND MOTIVATION

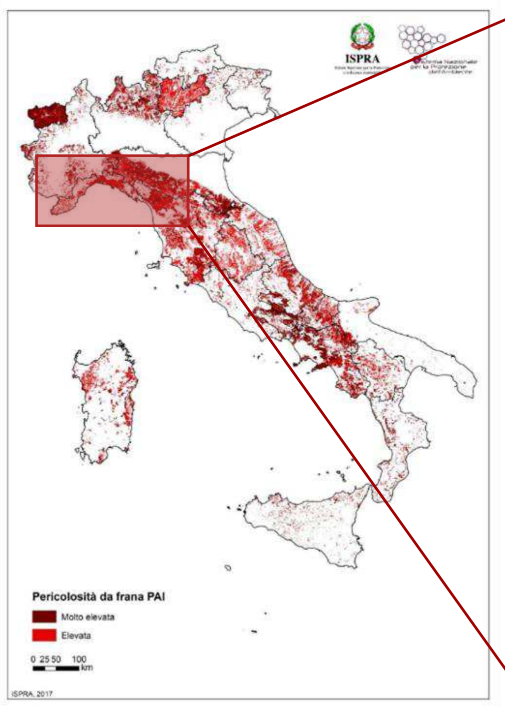

Landslide susceptibility (2018)

Liguria region, Italy

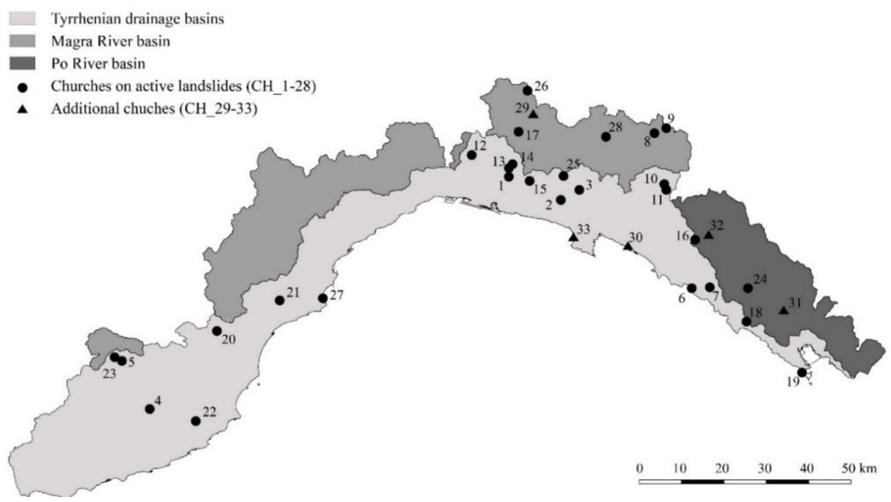

- **58.1%** of the territory affected by landslides

PRIN PERICLES Project 2015

Protecting the Cultural Heritage from water-soil interaction related threats

Ferrero C, Cambiaggi L, Vecchiattini R, Calderini C. (2021) Damage assessment of historic masonry churches exposed to slow-moving. *International Journal of Architectural Heritage,* 15(8): 1170-1195.

BACKGROUND AND MOTIVATION

- Vulnerability of masonry arches to slow-moving landslides

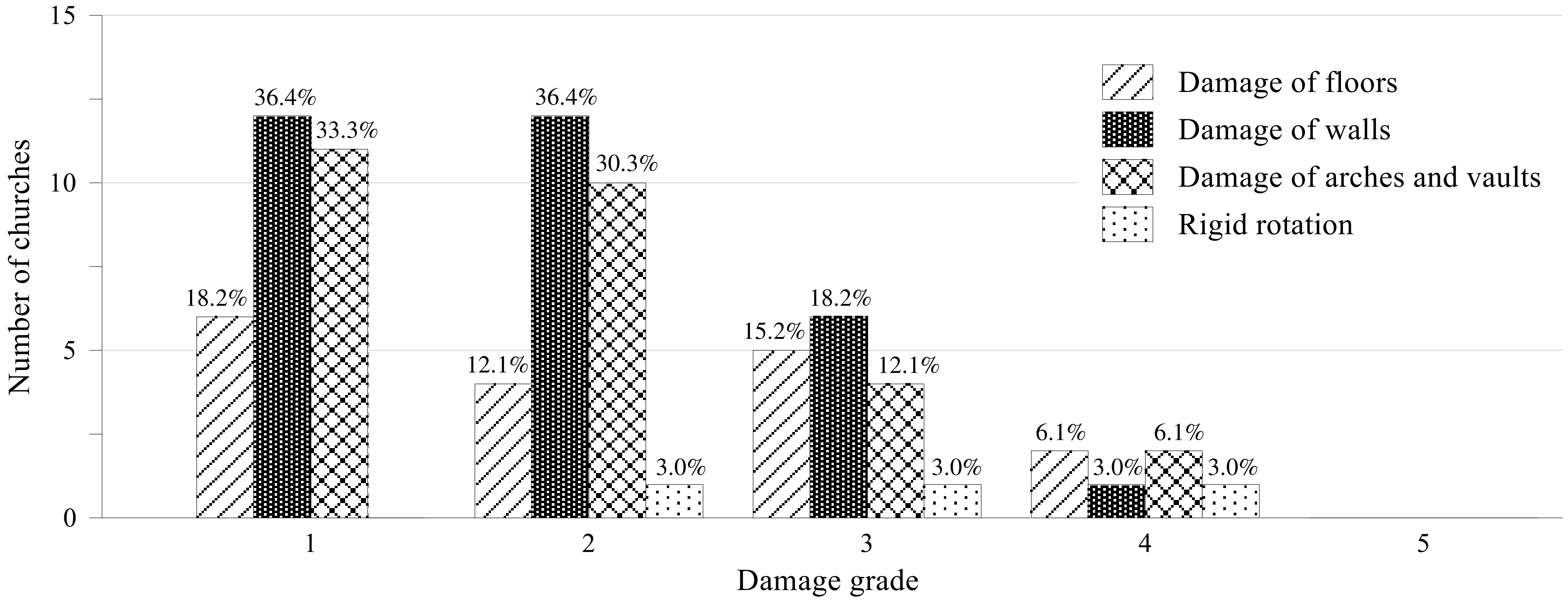

Damage grade: 1 – negligible to slight damage; 2 – moderate damage; 3- substantial to heavy damage; 4 – very heavy damage; 5- destruction

BACKGROUND AND MOTIVATION

- Vulnerability of masonry arches to slow-moving landslides

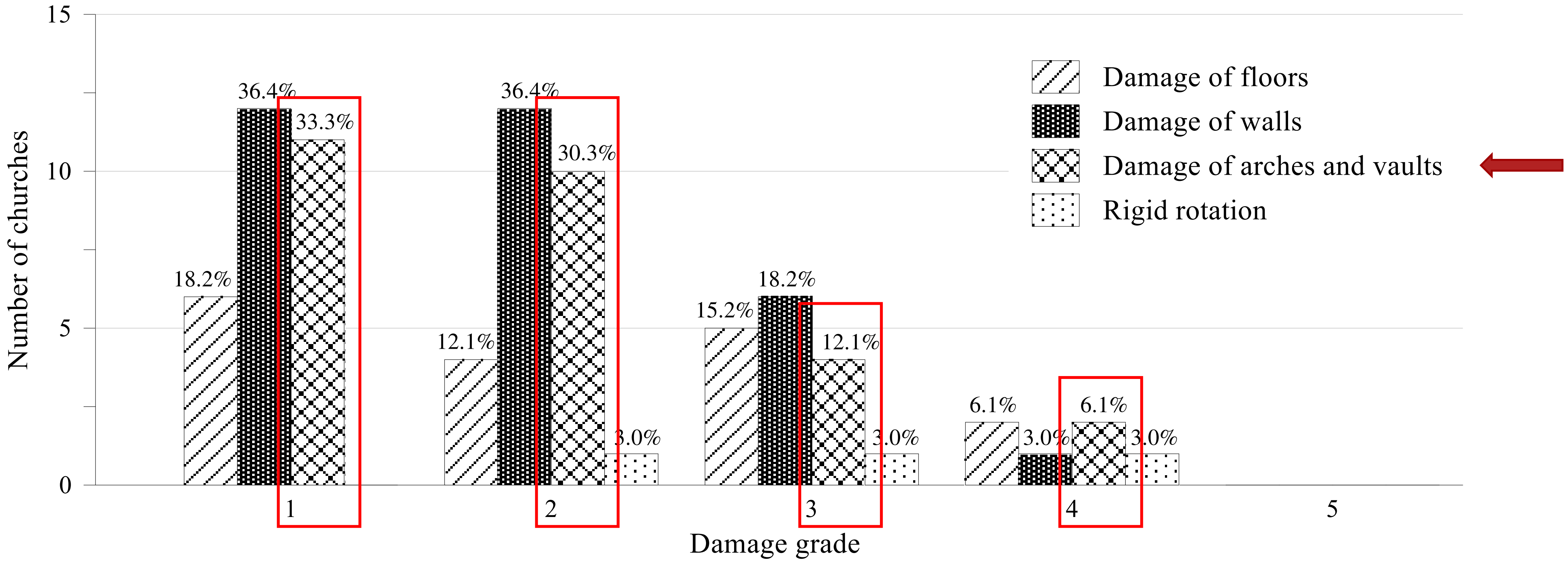

Damage grade: 1 – negligible to slight damage; 2 – moderate damage; 3- substantial to heavy damage; 4 – very heavy damage; 5- destruction

BACKGROUND AND MOTIVATION

- Lack of detailed studies dealing with inclined support displacements

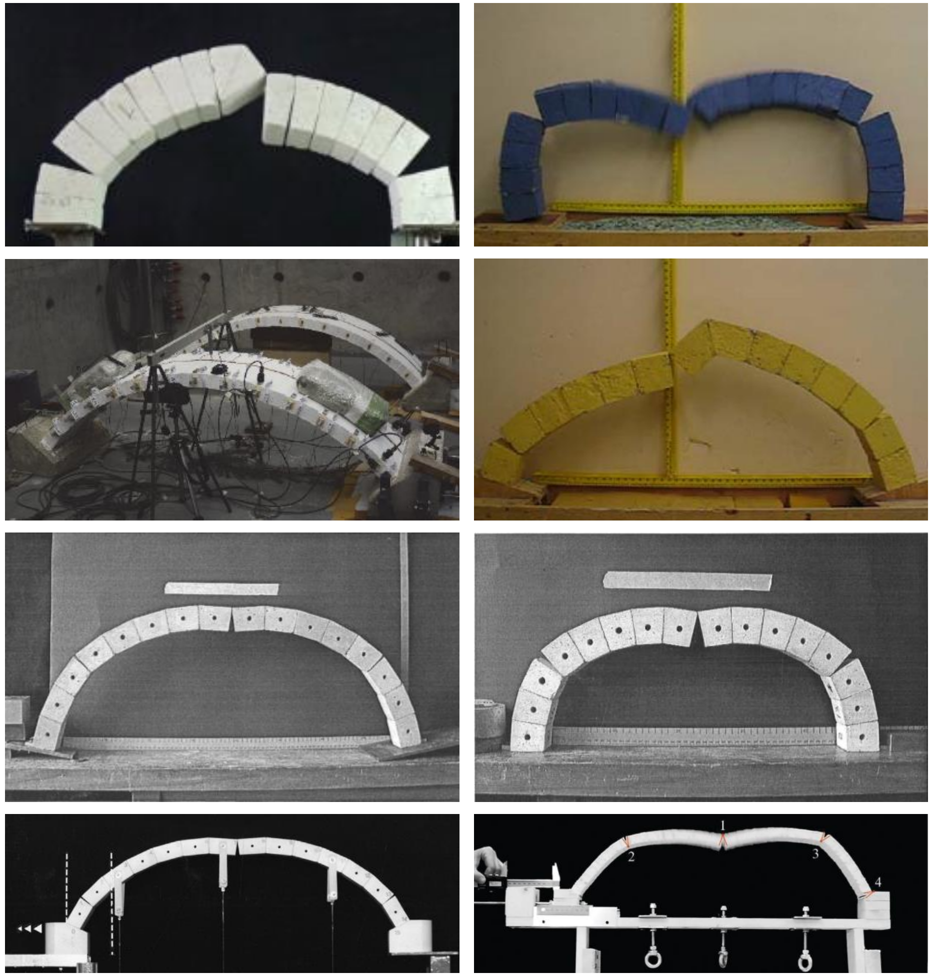

Horizontal displacements

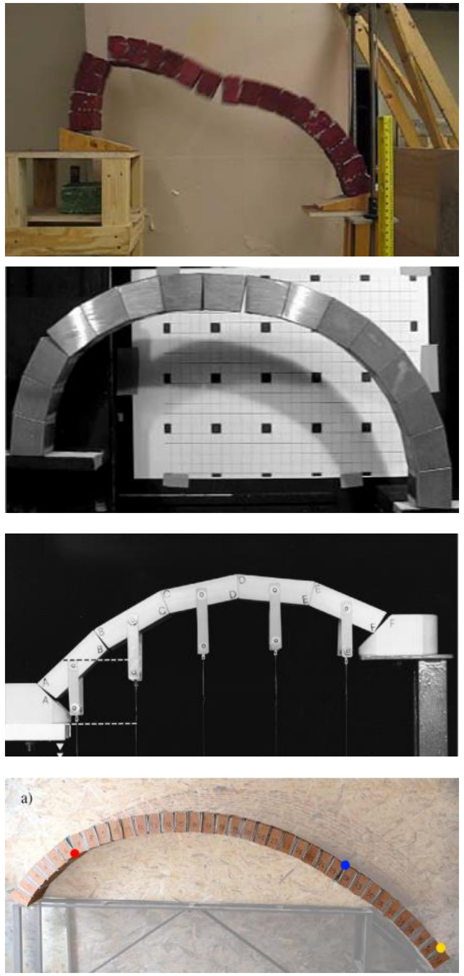

Vertical displacements

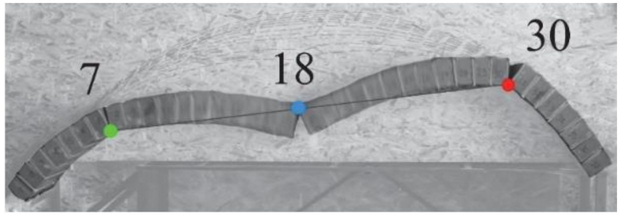

Inclined displacements

Ochsendorf, 2006; Romano and Ochsendorf, 2010; Romano, 2005; Galassi et al., 2018; Zampieri et al., 2018; Smars, 2010; Masciotta et al., 2020

BACKGROUND AND MOTIVATION

- Difficulty in correctly assessing the structural safety of masonry arches on moving supports by using analytical/numerical models

Galassi et al., 2018

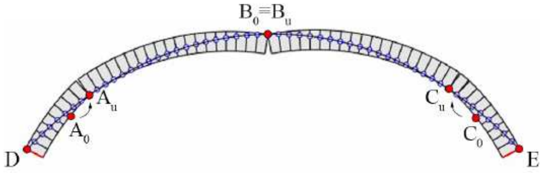

Ferrero et al., 2021

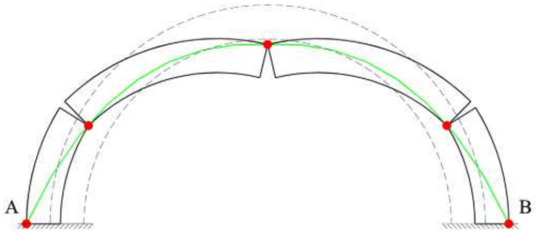

Coccia et al., 2015

Rigid-no tension models complying with Heyman's assumptions of Limit Analysis:

- infinite compressive strength
- zero tensile strength
- no sliding failure

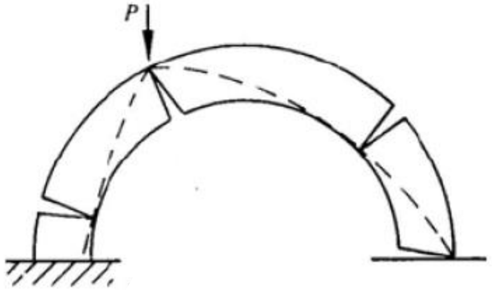

Heyman J., 1995

BACKGROUND AND MOTIVATION

- Difficulty in correctly assessing the structural safety of masonry arches on moving supports by using analytical/numerical models

Galassi et al., 2018

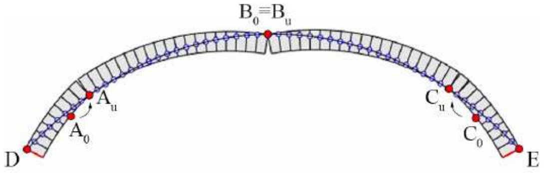

Ferrero et al., 2021

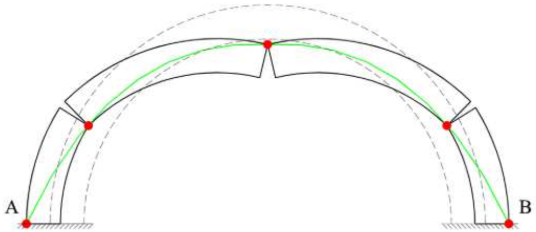

Coccia et al., 2015

Rigid-no tension models complying with Heyman's assumptions of Limit Analysis:

- infinite compressive strength
- zero tensile strength
- no sliding failure

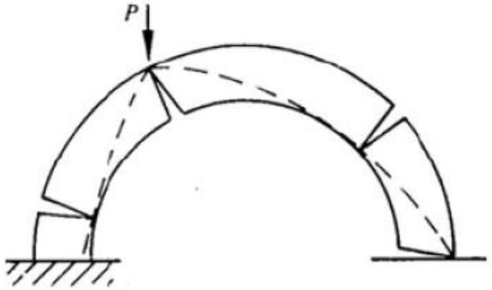

Heyman J., 1995

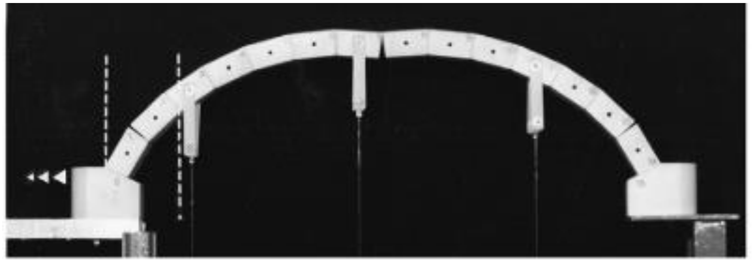

δ_c = 41.7 mm

Galassi et al., 2018

δ_c = 48.5 mm

Overestimation of the ultimate displacement capacity obtained experimentally

OBJECTIVES AND METHODOLOGY

Objectives

- To provide a full understanding of the **response of masonry arches to inclined support displacements**.
- To **understand why rigid-no tension models fail** in accurately predicting the actual response of dry-joint masonry arches to large support displacements.
- To **propose a numerical modelling approach** able to obtain a better matching between experimental and numerical responses.

Methodology

- **Experimental tests** on a small-scale dry-joint masonry arch subjected to vertical, horizontal and inclined support displacements
- **Numerical simulations** of the experimental tests adopting a finite element micro-modelling approach

EXPERIMENTAL TESTS

- **Physical model**

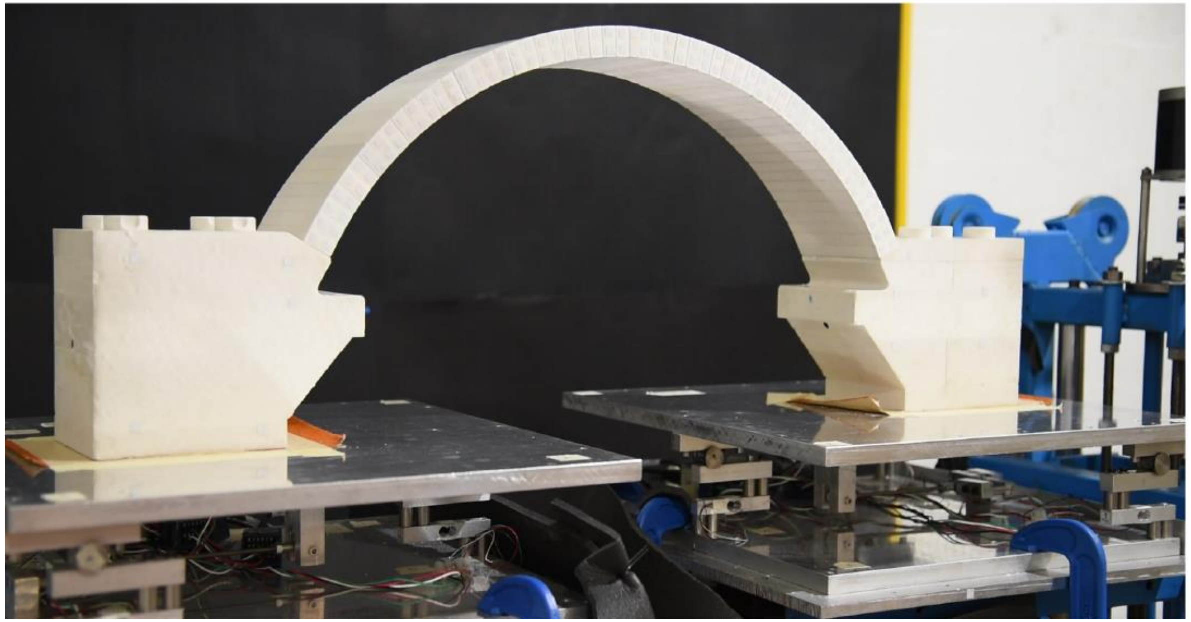

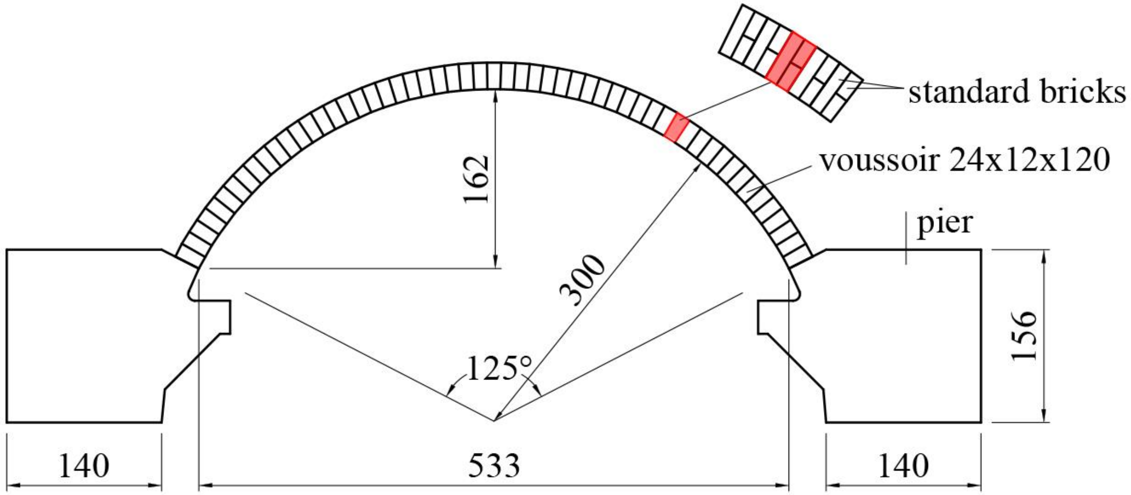

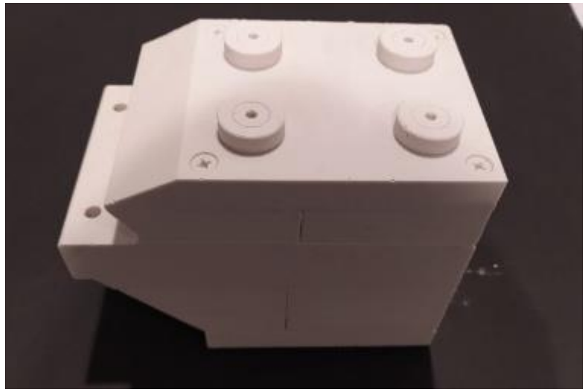

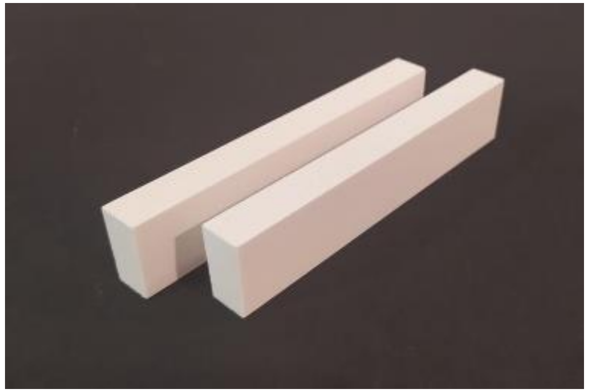

E [MPa]	σ_c [MPa]	Φ [°]	ρ [kg/m^3]
941	9.1	41.2	1640

EXPERIMENTAL TESTS

- **Application of support displacements**

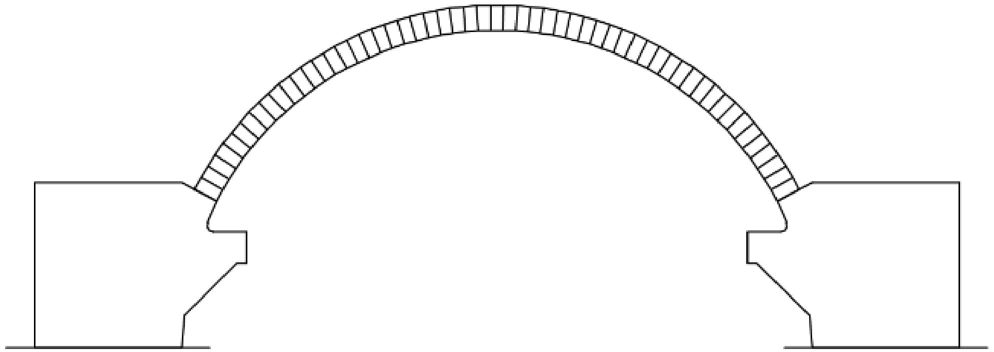

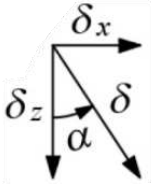

α[°]	0	5	10	15	20	25	30	35	40	45	60	75	90

13 combinations of **vertical** and **horizontal** support displacements

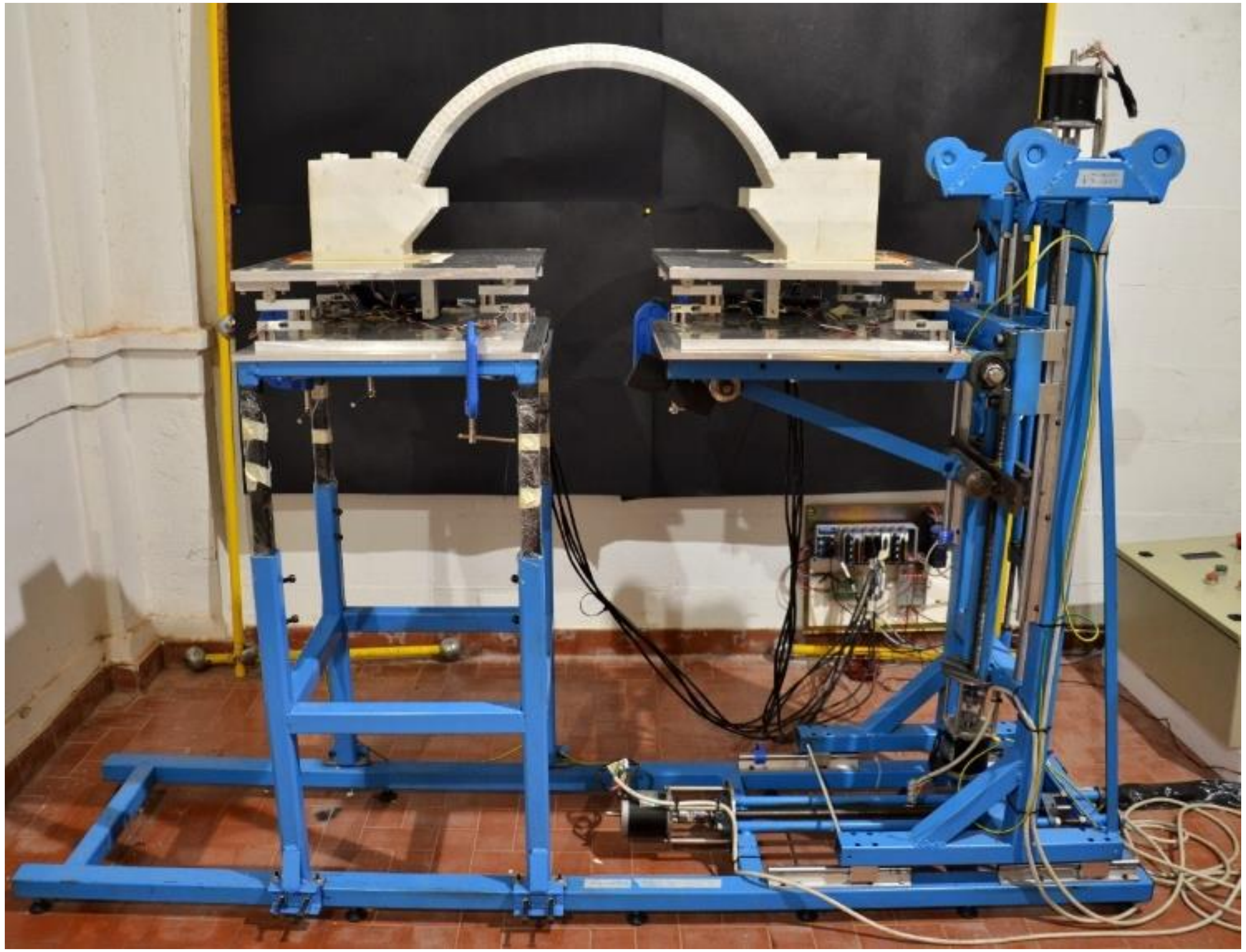

EXPERIMENTAL TESTS

- **Collapse mechanisms and modes of evolution of the hinge configuration**

$\alpha = 0° \div 15°$

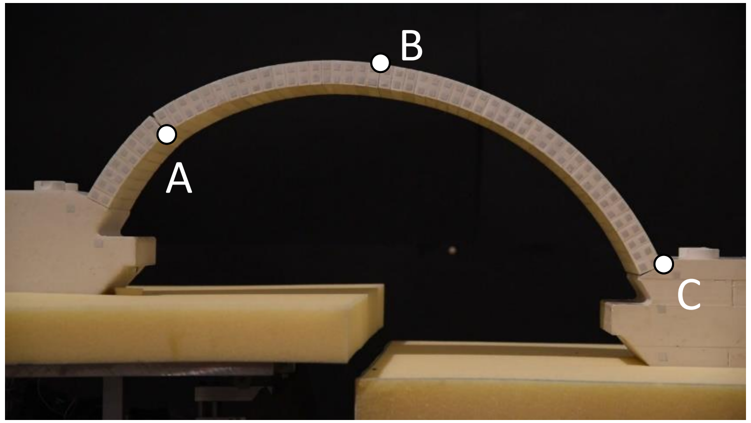

Initial sequence: I-E-E

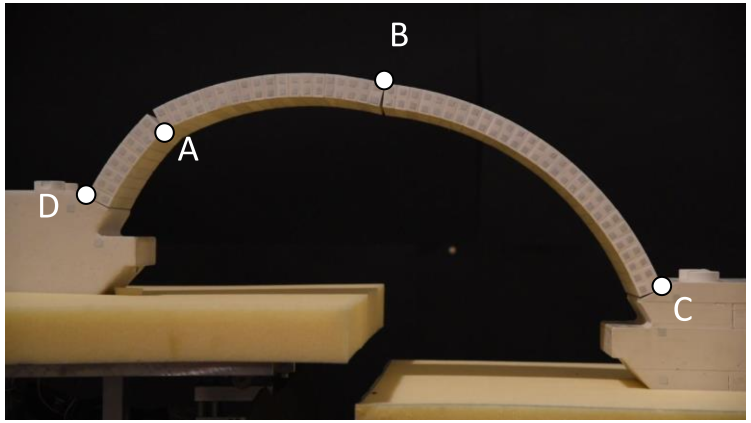

Final sequence: E-I-E-E

$\alpha = 20°$

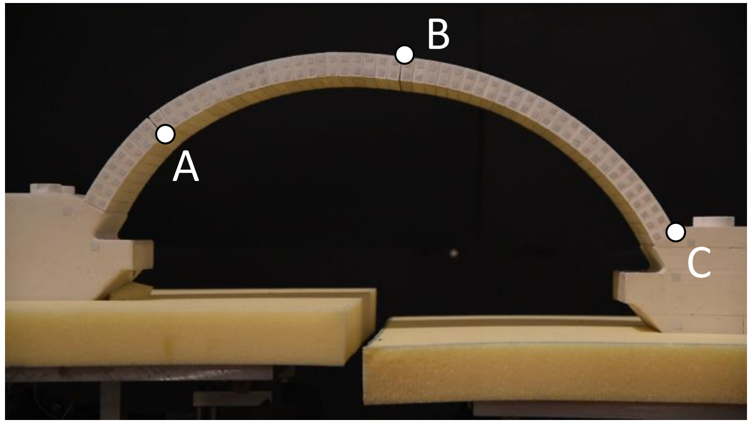

Initial sequence: I-E-E

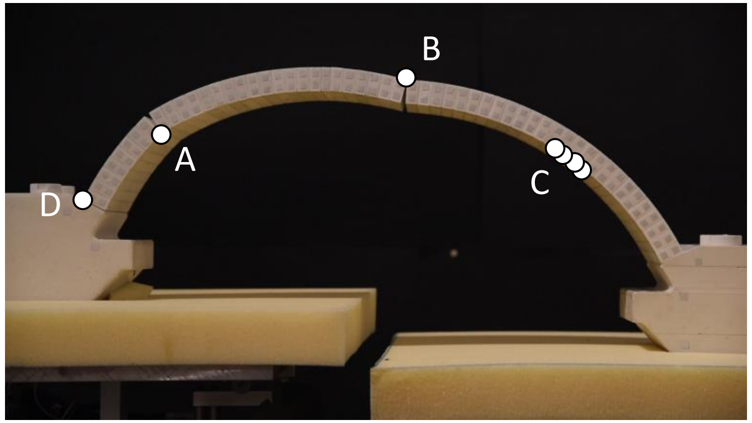

Final sequence: E-I-E-I

$\alpha = 25° \div 90°$

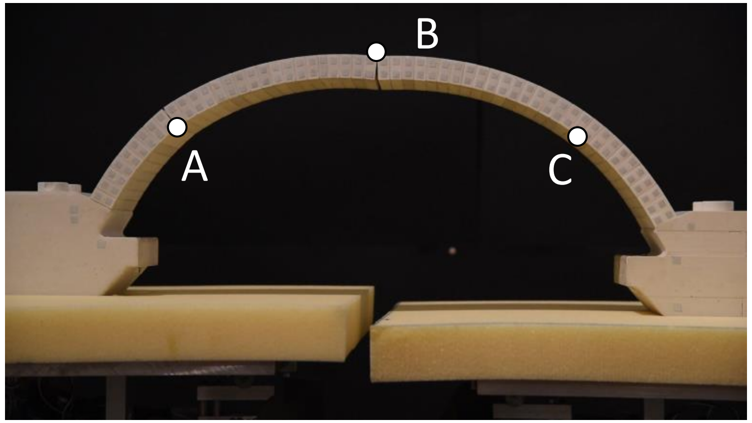

Initial sequence: I-E-I

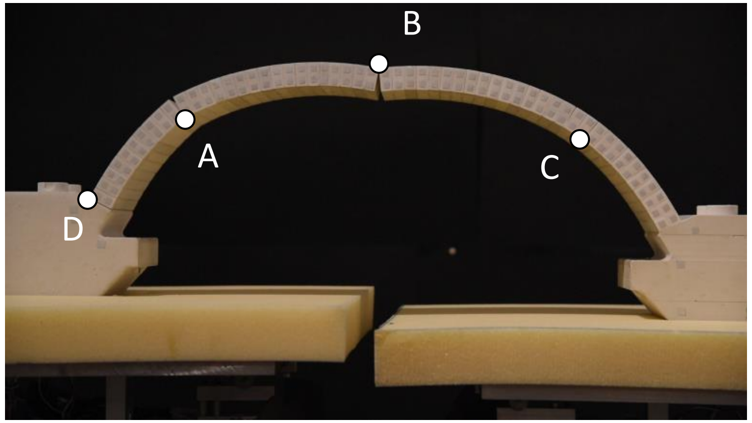

Final sequence: E-I-E-I/E-I-E-I-E

EXPERIMENTAL TESTS

- **Collapse mechanisms and modes of evolution of the hinge configuration**

MODE I

$\alpha = 0°\div 15°$

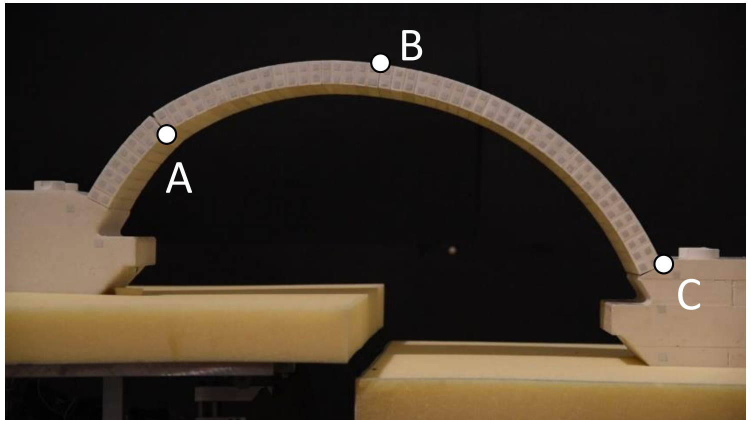

Initial sequence: I-E-E

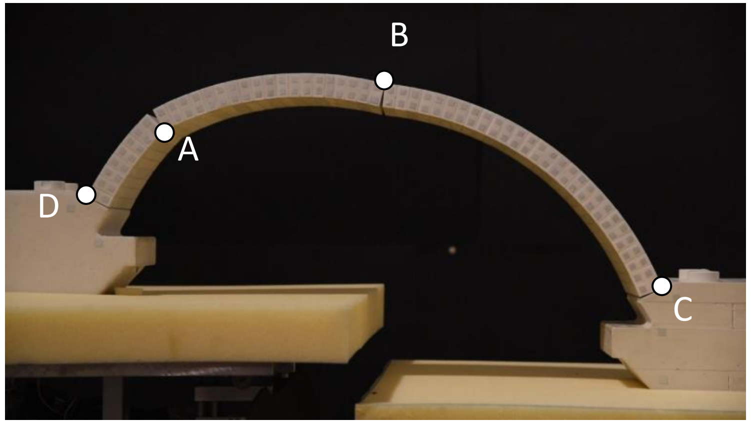

Final sequence: E-I-E-E

$\alpha = 20°$

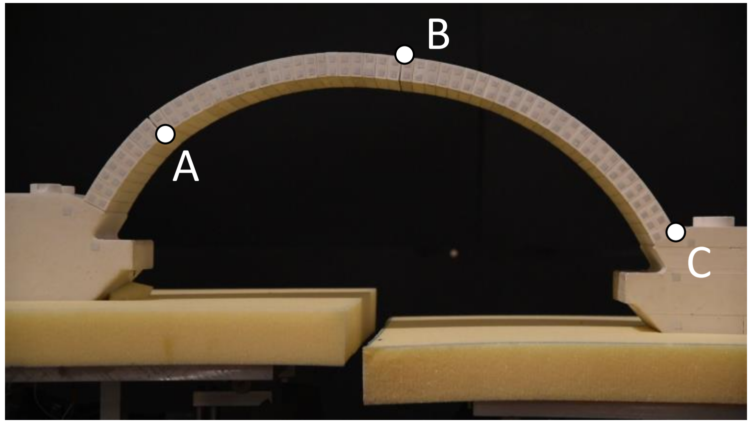

Initial sequence: I-E-E

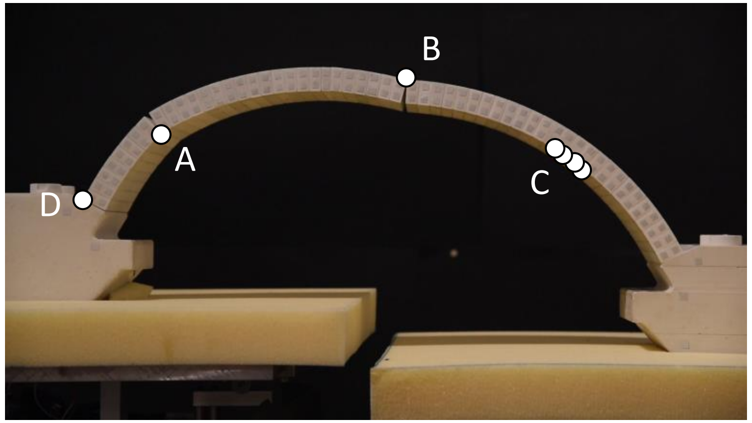

Final sequence: E-I-E-I

$\alpha = 25°\div 90°$

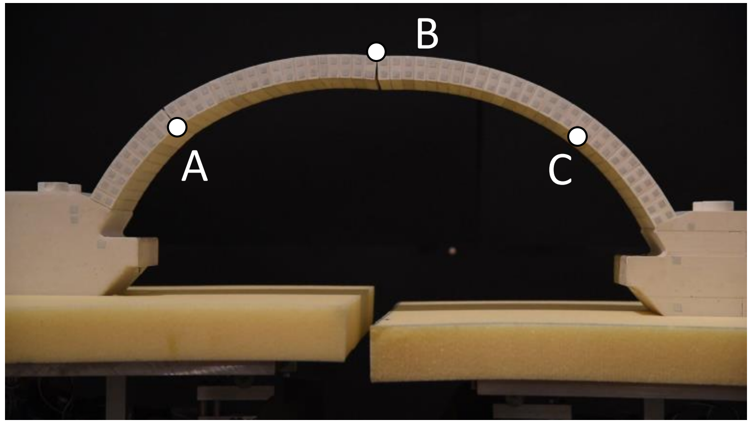

Initial sequence: I-E-I

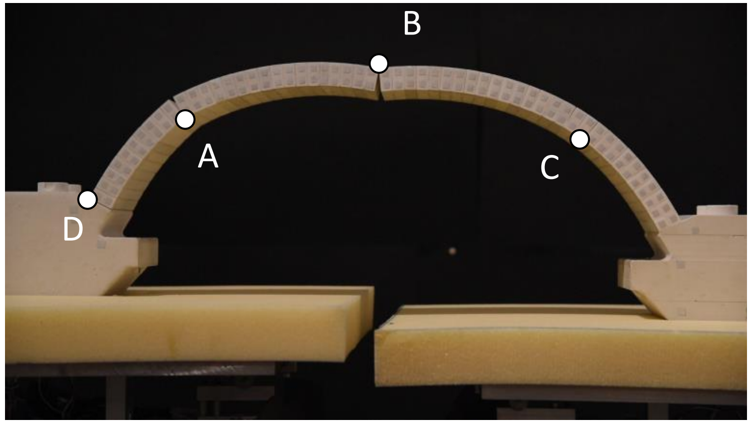

Final sequence: E-I-E-I/E-I-E-I-E

EXPERIMENTAL TESTS

- **Collapse mechanisms and modes of evolution of the hinge configuration**

MODE I

$\alpha = 0°÷15°$

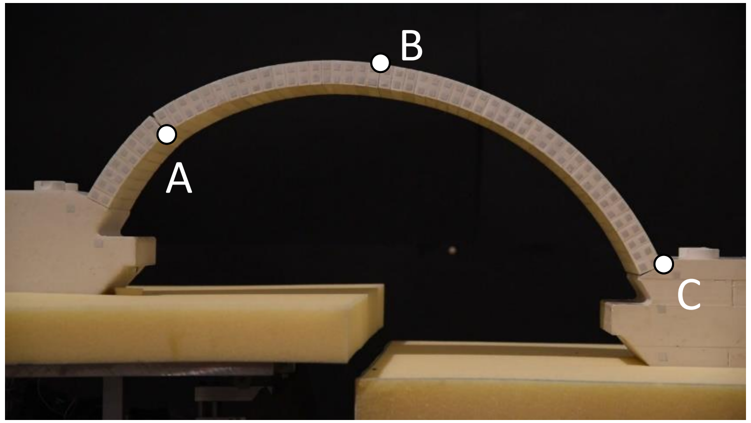

Initial sequence: I-E-E

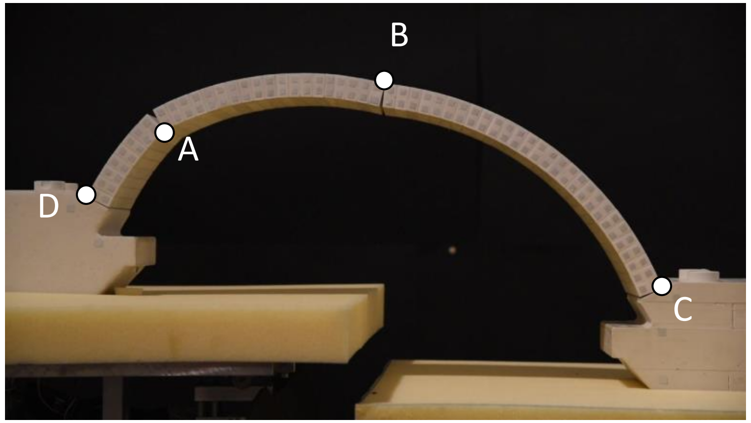

Final sequence: E-I-E-E

MODE II

$\alpha = 20°$

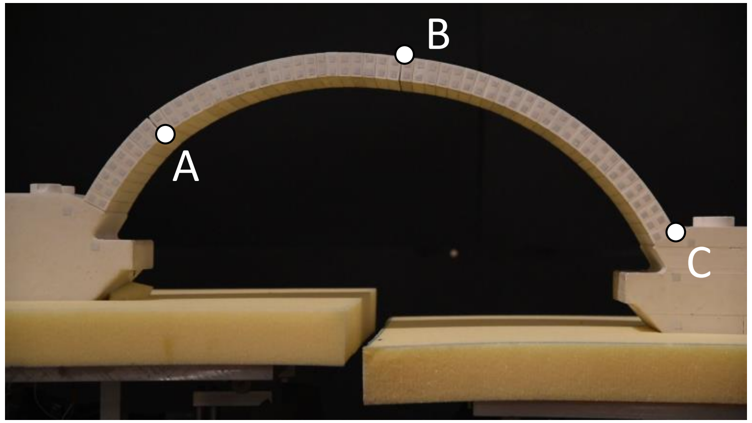

Initial sequence: I-E-E

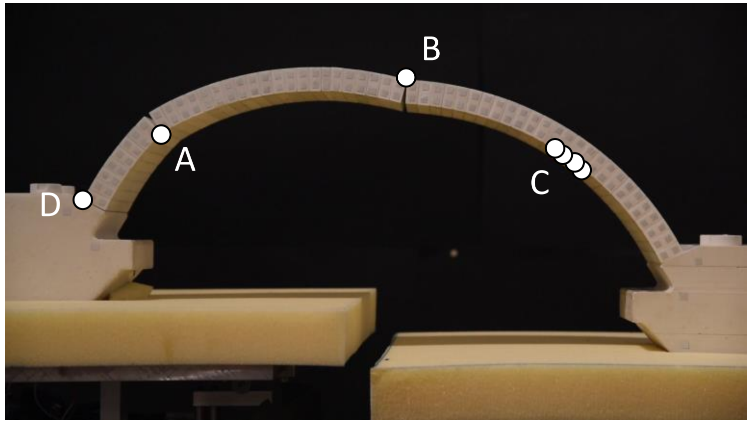

Final sequence: E-I-E-I

$\alpha = 25°÷90°$

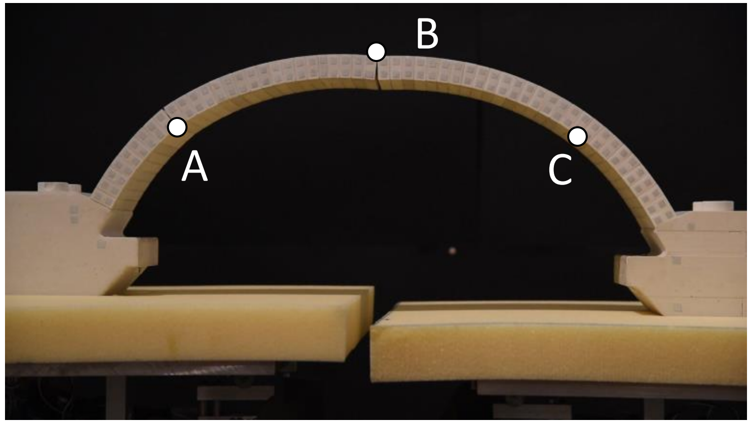

Initial sequence: I-E-I

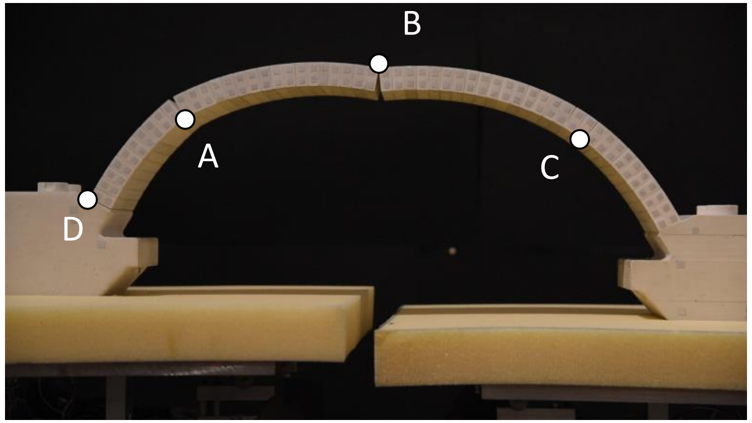

Final sequence: E-I-E-I/E-I-E-I-E

EXPERIMENTAL TESTS

- **Collapse mechanisms and modes of evolution of the hinge configuration**

MODE I

$\alpha = 0° \div 15°$

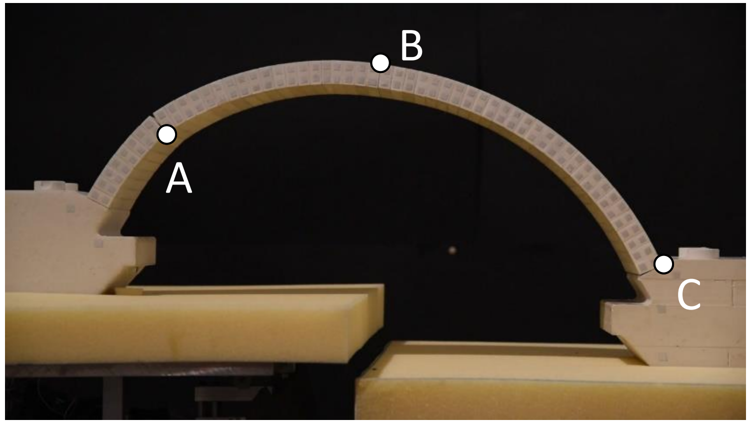

Initial sequence: I-E-E

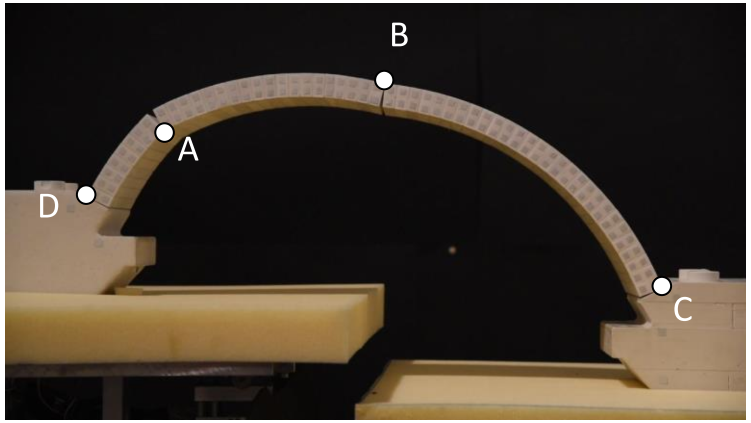

Final sequence: E-I-E-E

MODE II

$\alpha = 20°$

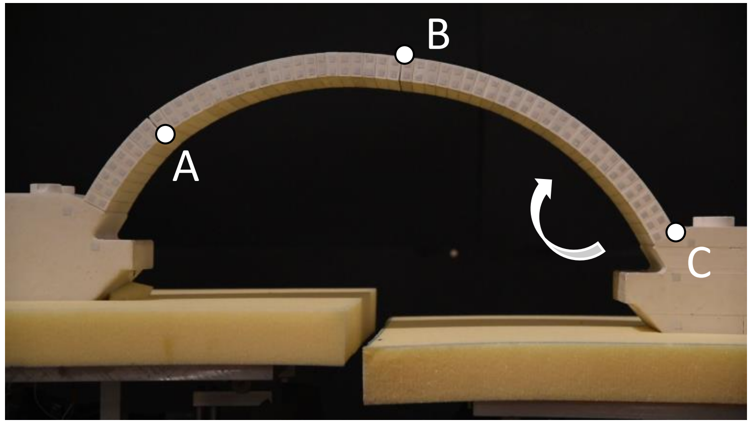

Initial sequence: I-E-E

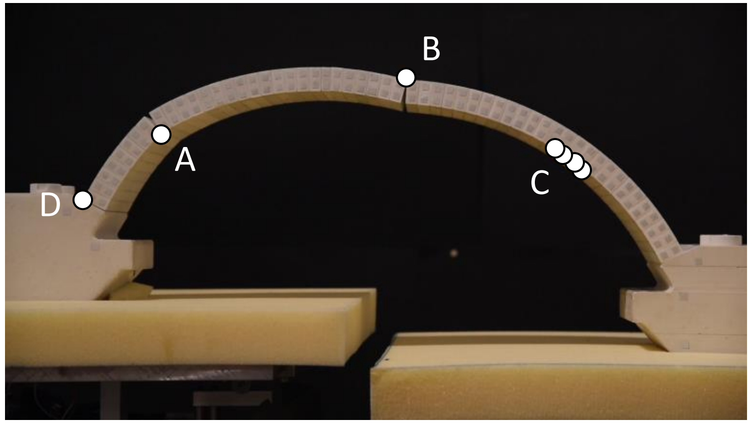

Final sequence: E-I-E-I

$\alpha = 25° \div 90°$

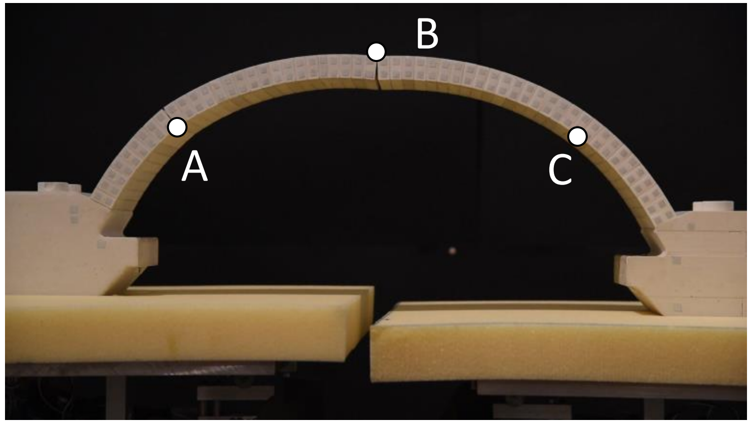

Initial sequence: I-E-I

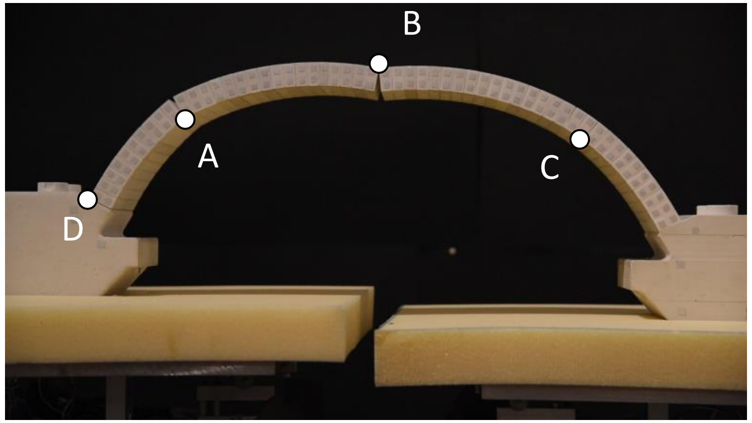

Final sequence: E-I-E-I/E-I-E-I-E

EXPERIMENTAL TESTS

- **Collapse mechanisms and modes of evolution of the hinge configuration**

MODE I

α = 0°÷15°

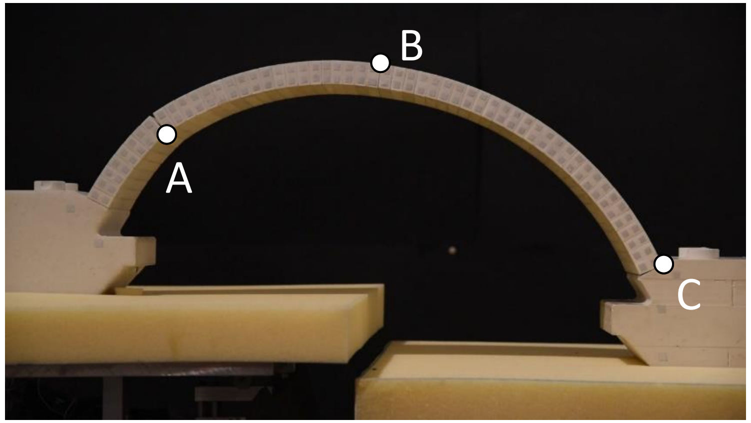

Initial sequence: I-E-E

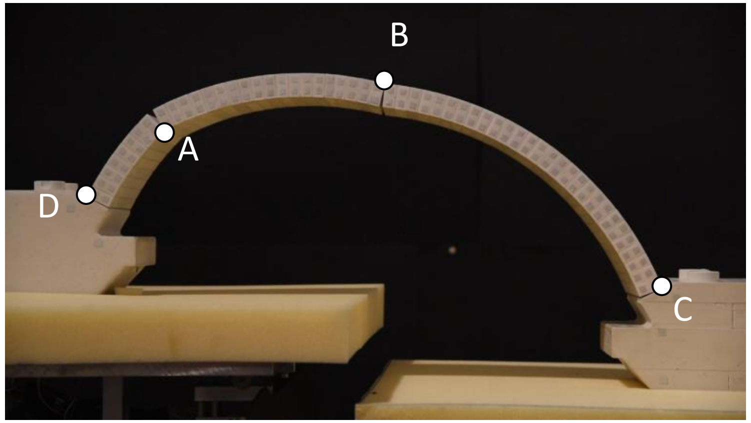

Final sequence: E-I-E-E

MODE II

α = 20°

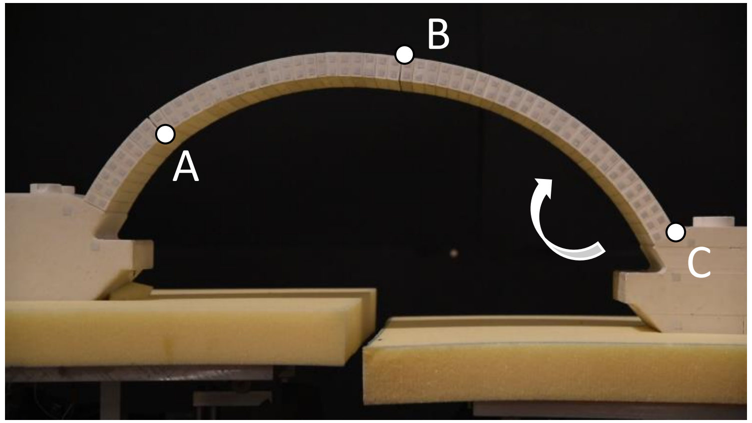

Initial sequence: I-E-E

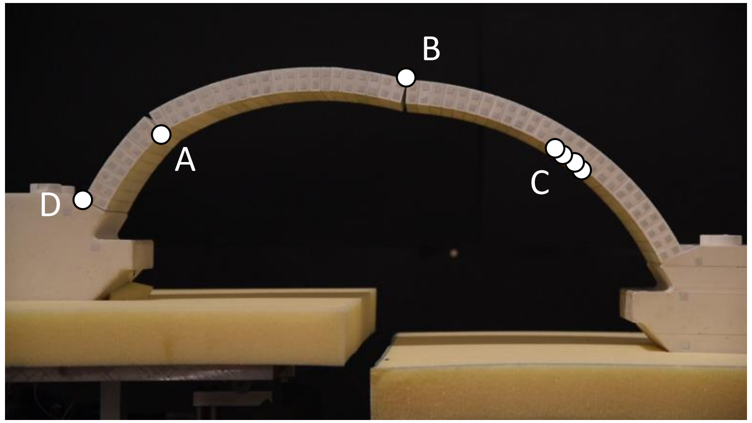

Final sequence: E-I-E-I

MODE III

α = 25°÷90°

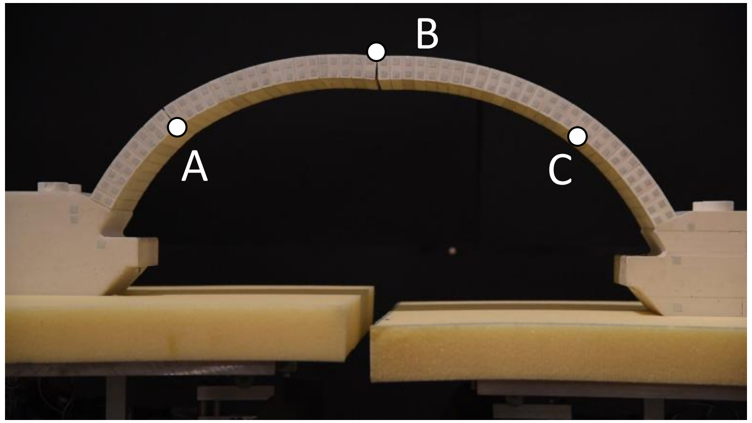

Initial sequence: I-E-I

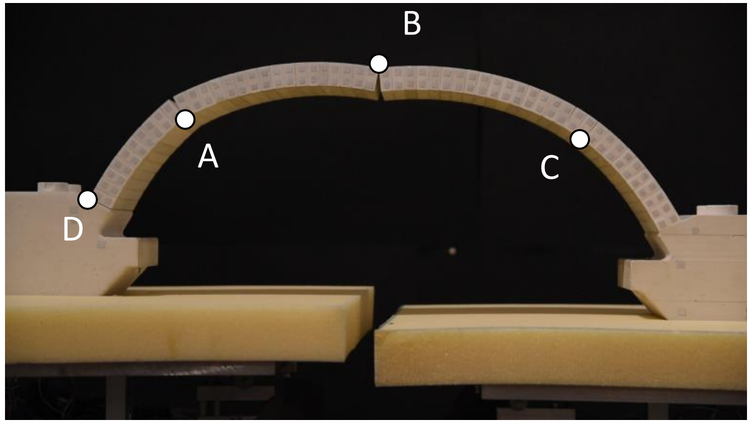

Final sequence: E-I-E-I/E-I-E-I-E

EXPERIMENTAL TESTS

- **Collapse mechanisms and modes of evolution of the hinge configuration**

MODE I

$\alpha = 0°÷15°$

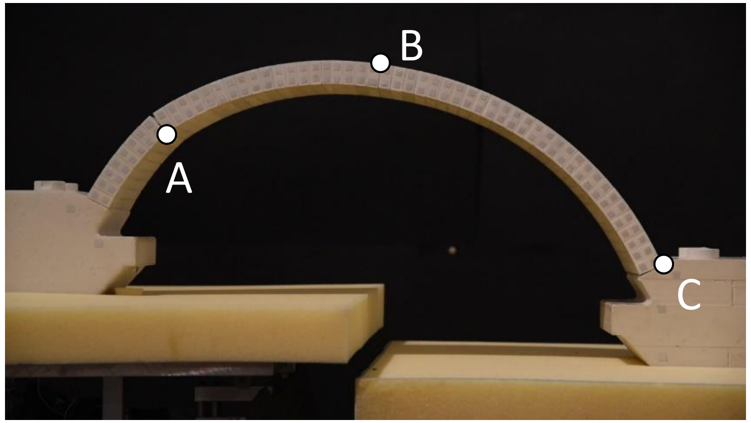

Initial sequence: I-E-E

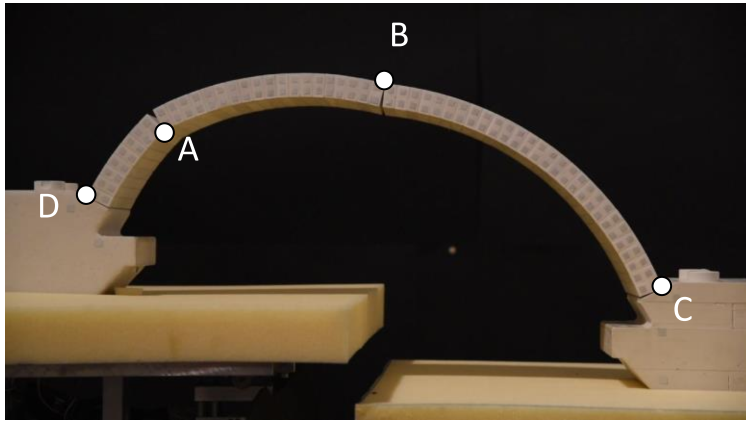

Final sequence: E-I-E-E

MODE II

$\alpha = 20°$

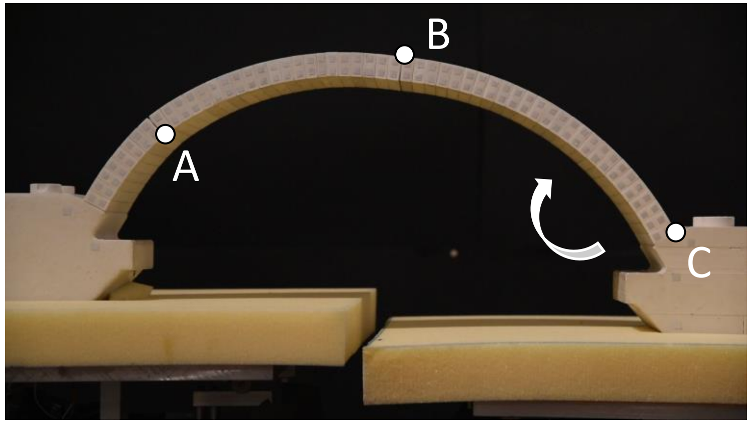

Initial sequence: I-E-E

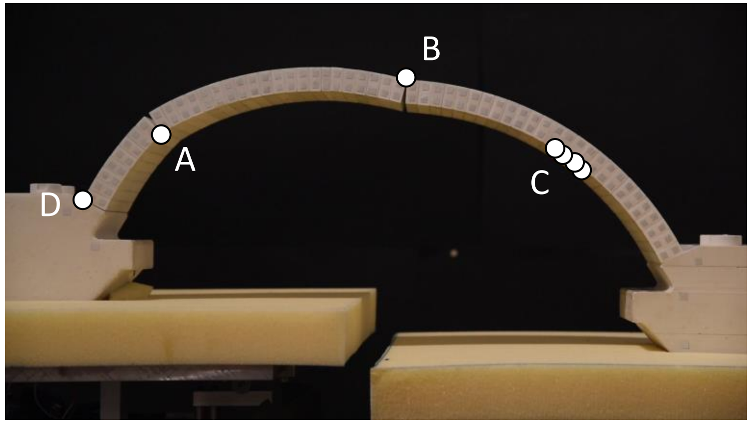

Final sequence: E-I-E-I

MODE III

$\alpha = 25°÷90°$

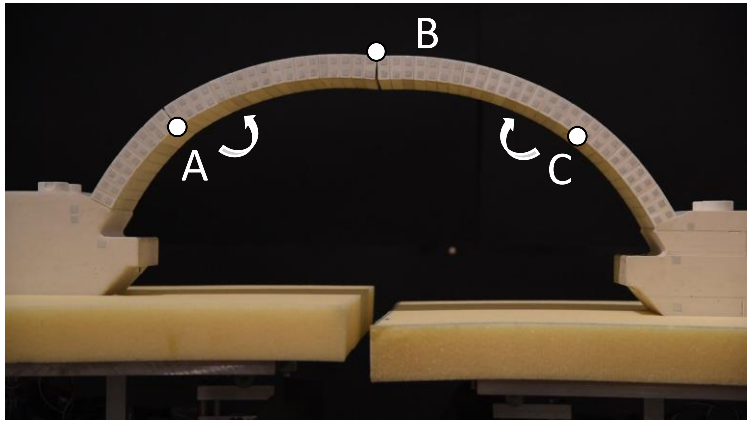

Initial sequence: I-E-I

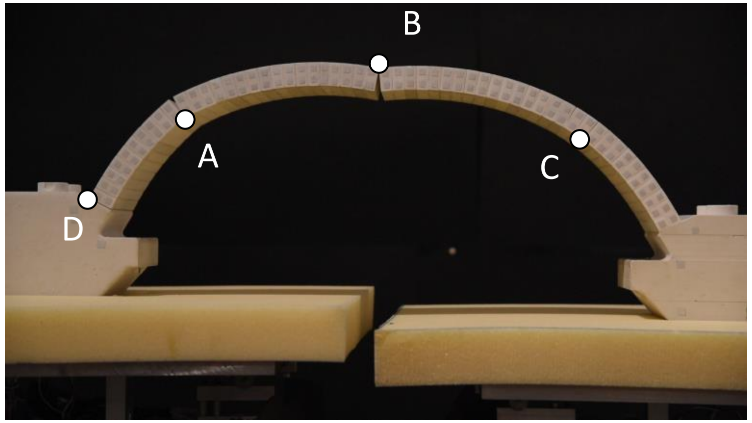

Final sequence: E-I-E-I/E-I-E-I-E

EXPERIMENTAL TESTS

- **Collapse mechanisms and modes of evolution of the hinge configuration**

MODE I

$\alpha = 0° \div 15°$

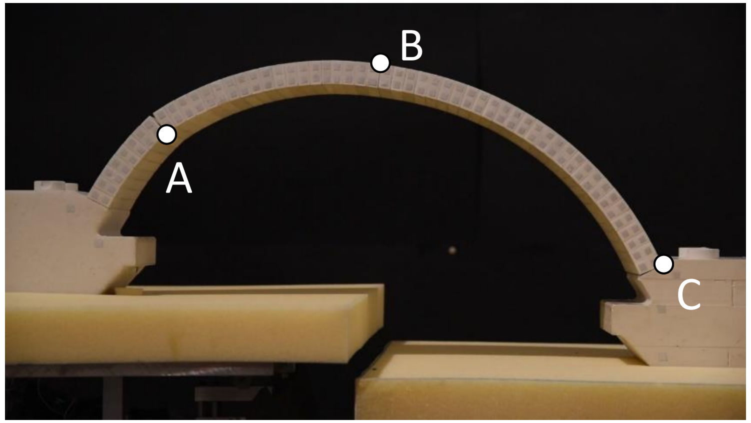

Initial sequence: I-E-E

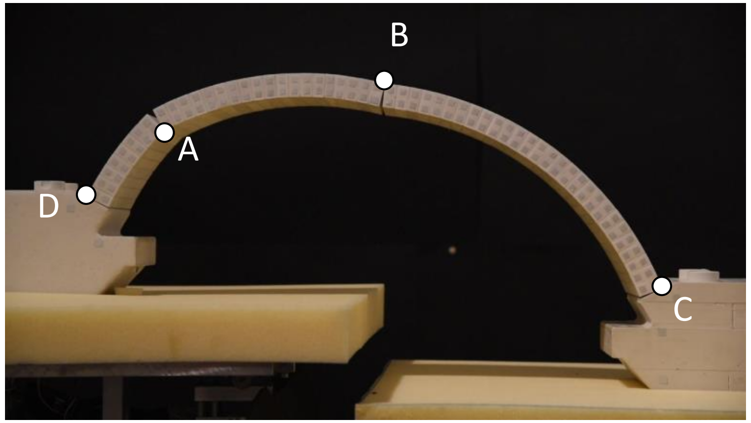

Final sequence: E-I-E-E

MODE II

$\alpha = 20°$

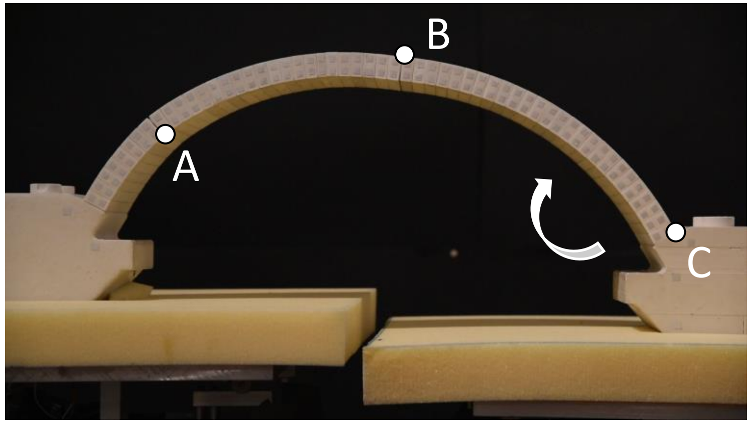

Initial sequence: I-E-E

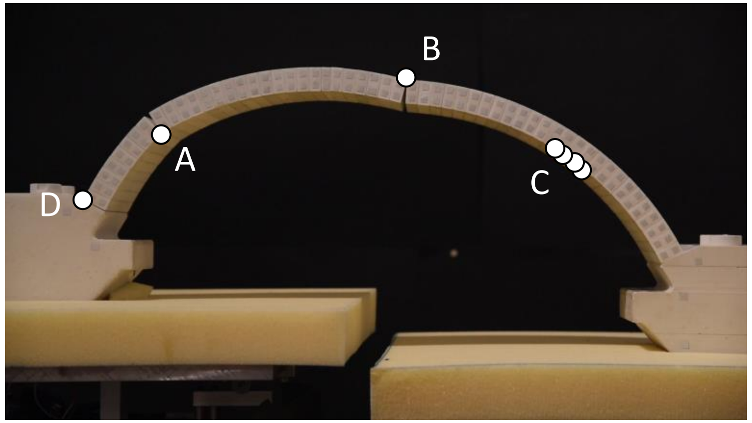

Final sequence: E-I-E-I

MODE III

$\alpha = 25° \div 90°$

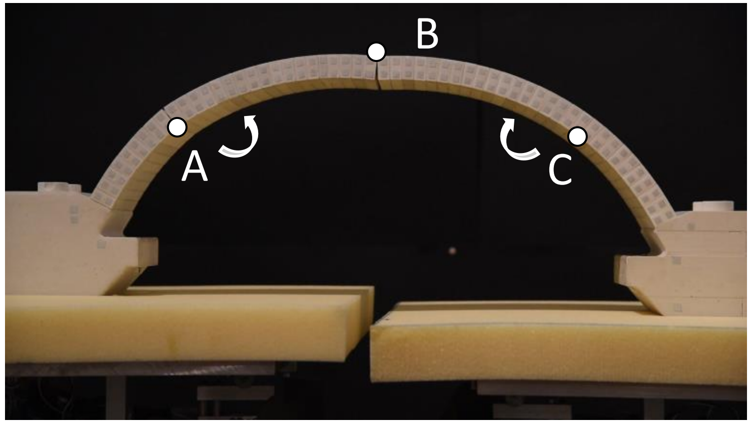

Initial sequence: I-E-I

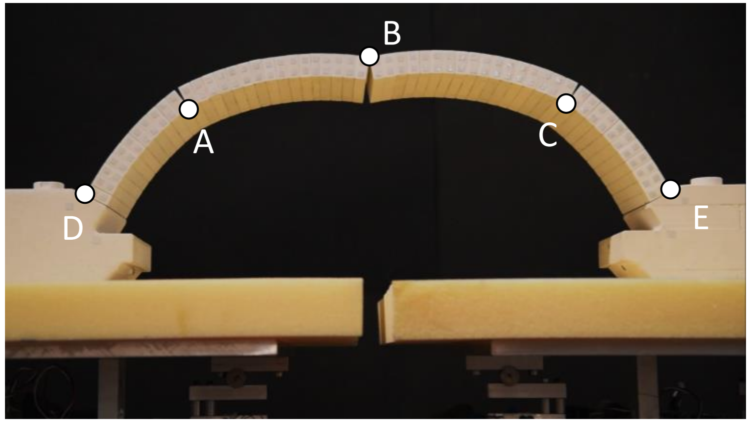

Final sequence: E-I-E-I/E-I-E-I-E

EXPERIMENTAL TESTS

- **Collapse displacements and limit displacement domain**

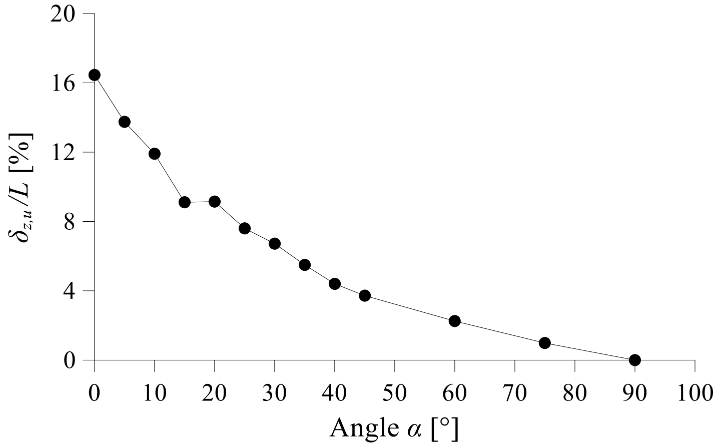

Vertical collapse displacement vs. α

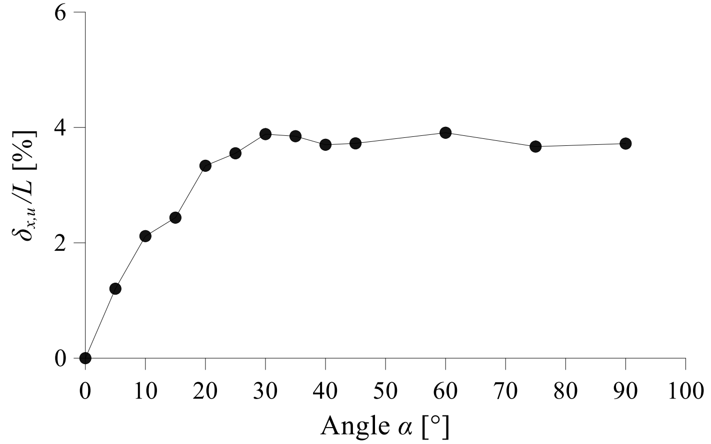

Horizontal collapse displacement vs. α

EXPERIMENTAL TESTS

- **Collapse displacements and limit displacement domain**

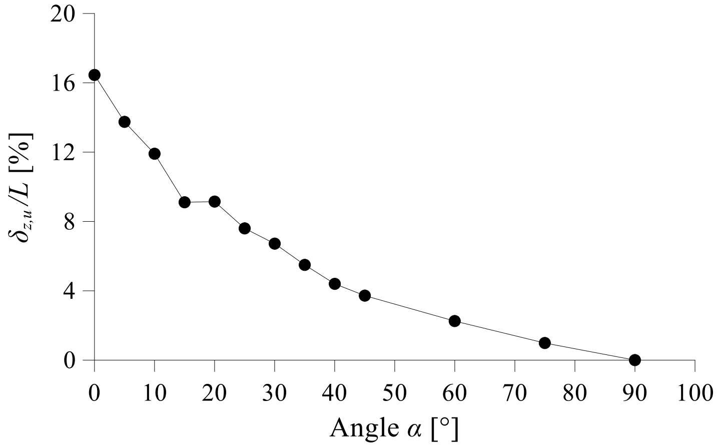

Vertical collapse displacement vs. α

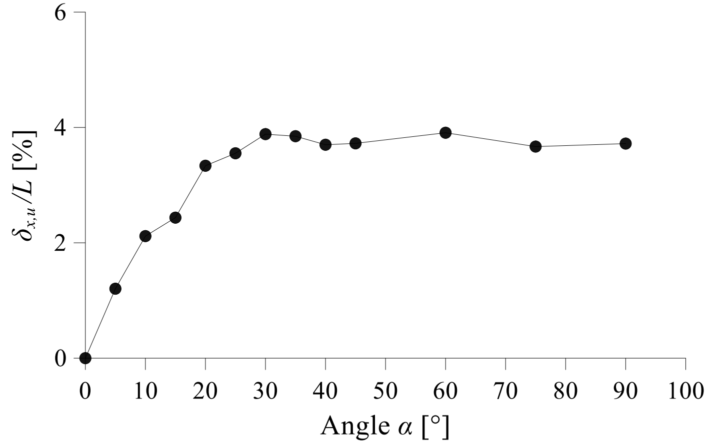

Horizontal collapse displacement vs. α

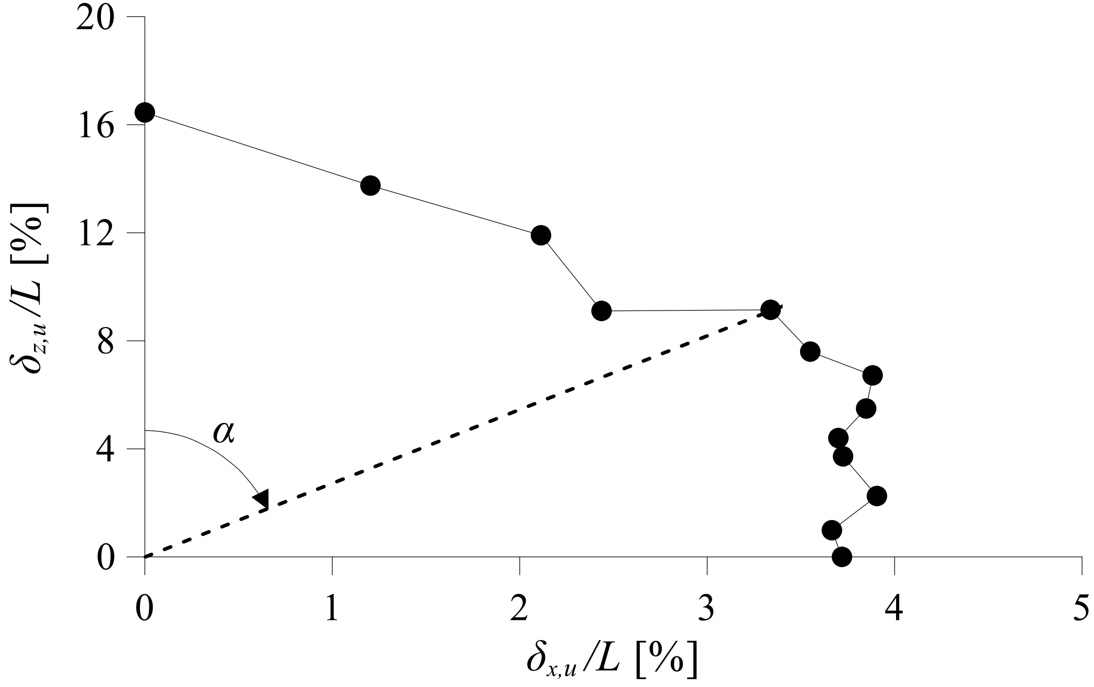

Limit displacement domain

EXPERIMENTAL TESTS

- **Collapse displacements and limit displacement domain**

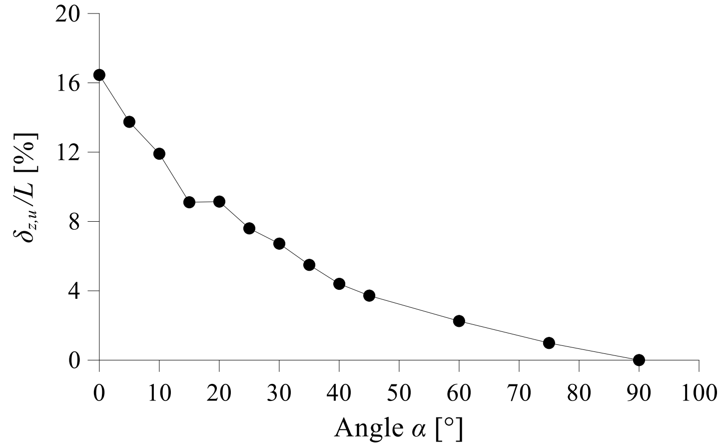

Vertical collapse displacement vs. α

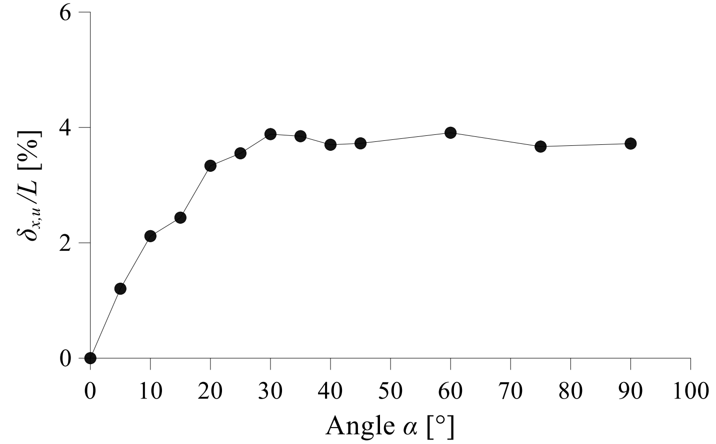

Horizontal collapse displacement vs. α

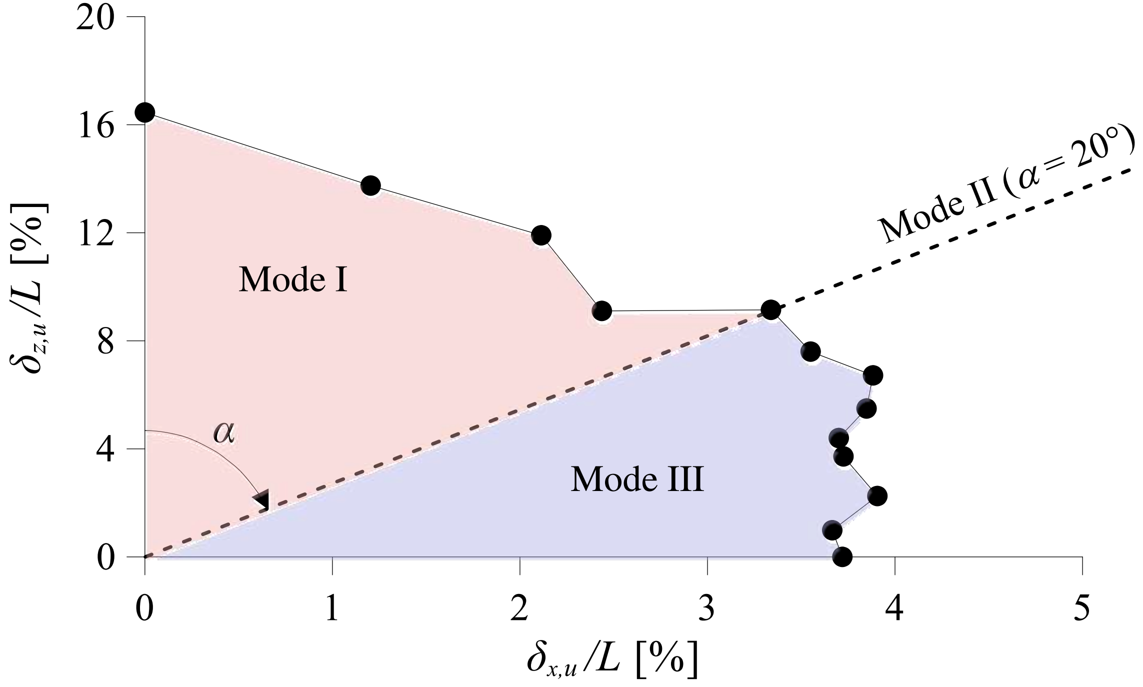

Limit displacement domain

EXPERIMENTAL TESTS

- **Graphic statics**

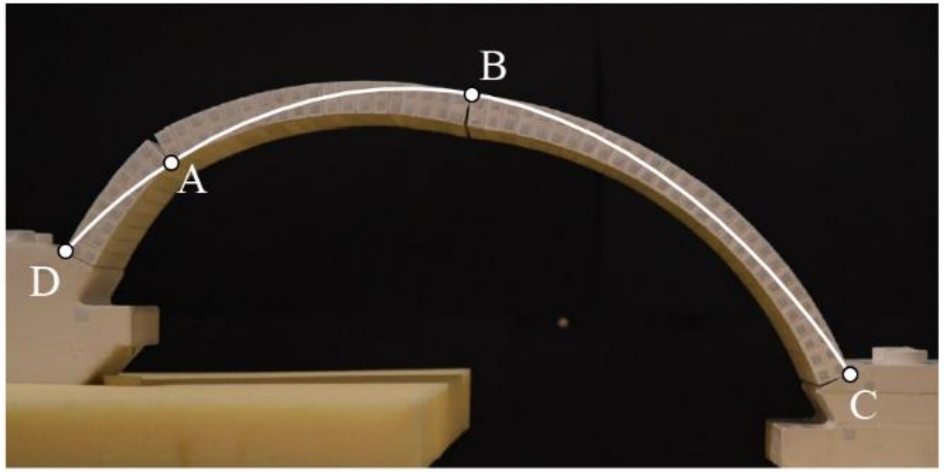

α = 0°-15°

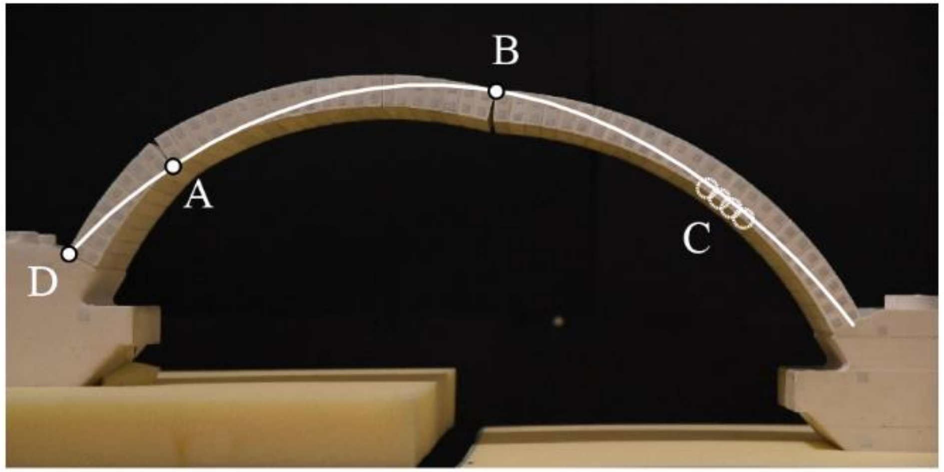

α = 20°-30°

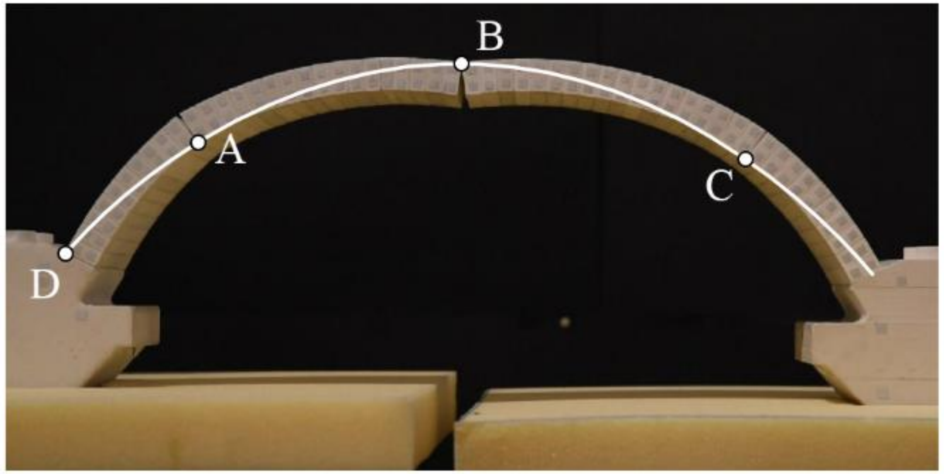

α = 35°-75°

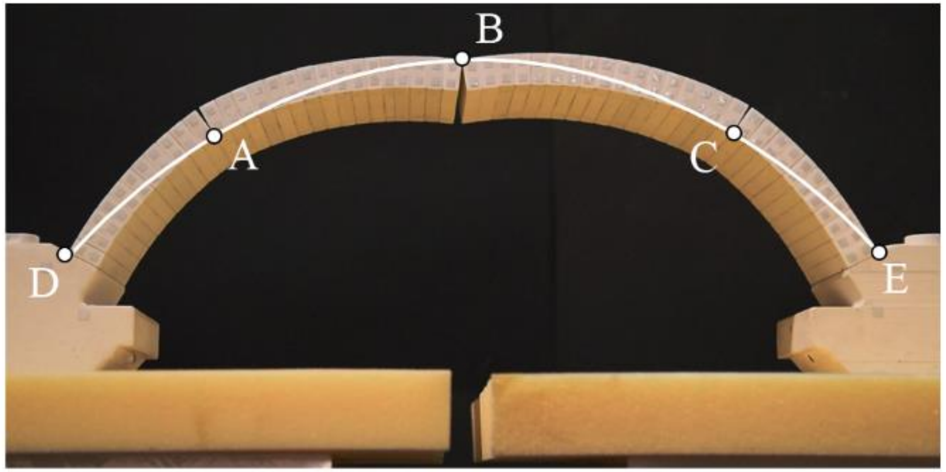

α = 90°

EXPERIMENTAL TESTS

- **Graphic statics**

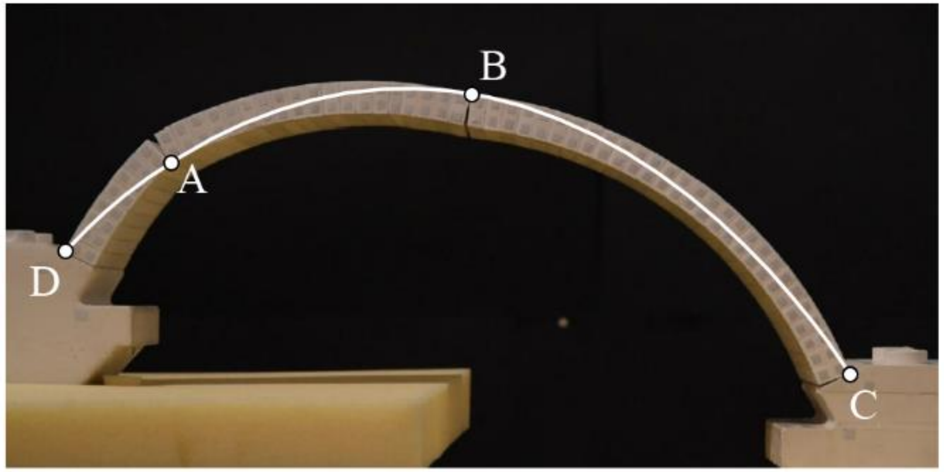

α = 0°-15°

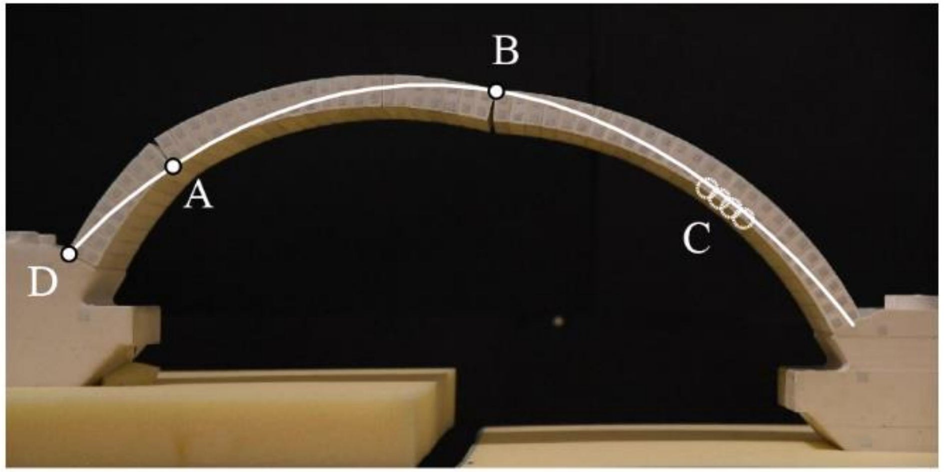

α = 20°-30°

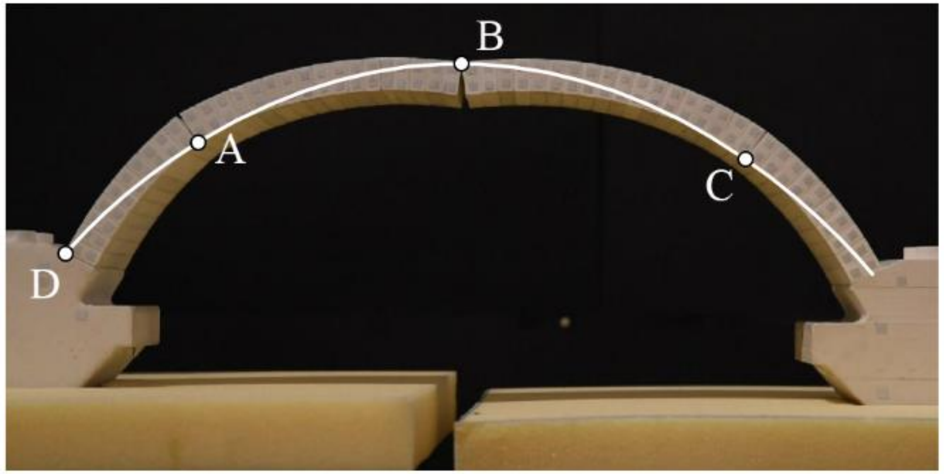

α = 35°-75°

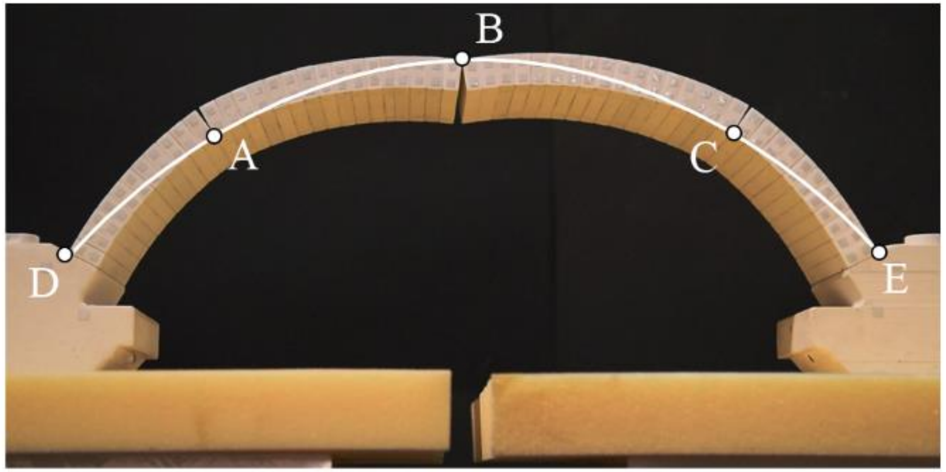

α = 90°

EXPERIMENTAL TESTS

- **Graphic statics**

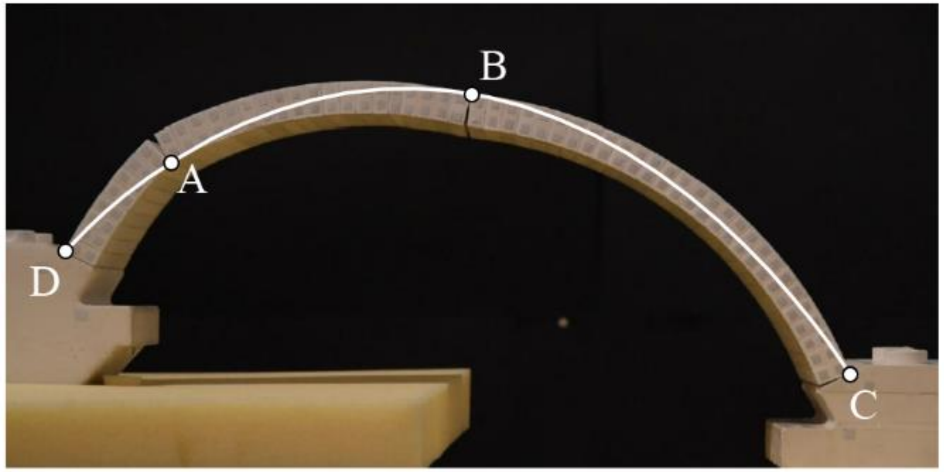

α = 0°-15°

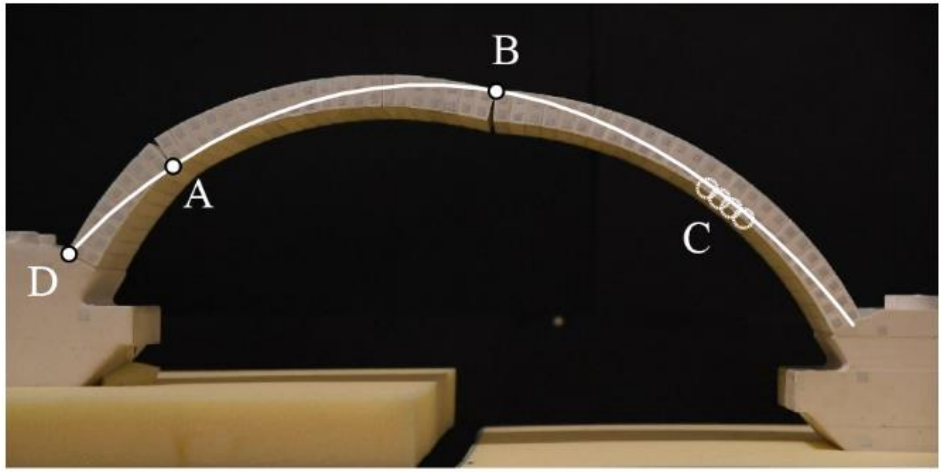

α = 20°-30°

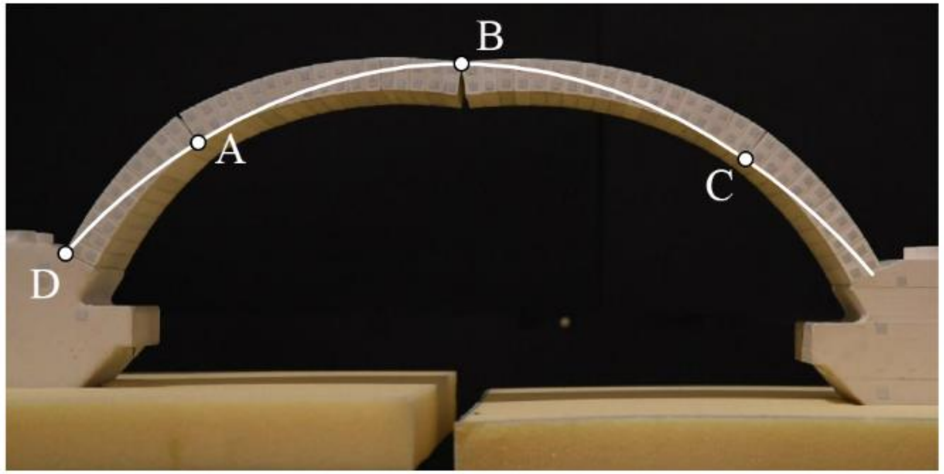

α = 35°-75°

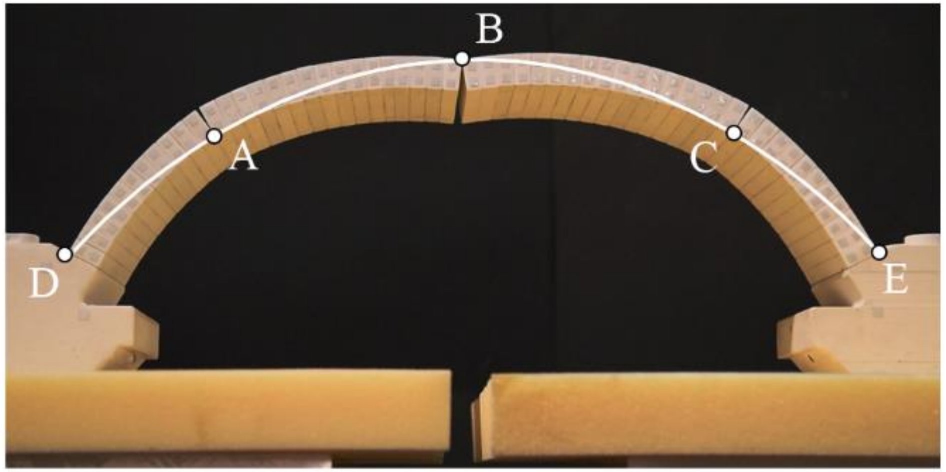

α = 90°

EXPERIMENTAL TESTS

- **Graphic statics**

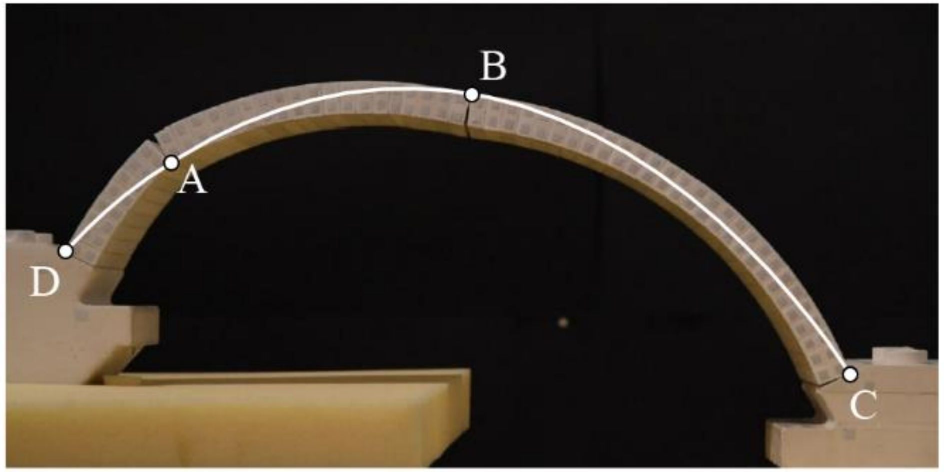

α = 0°-15°

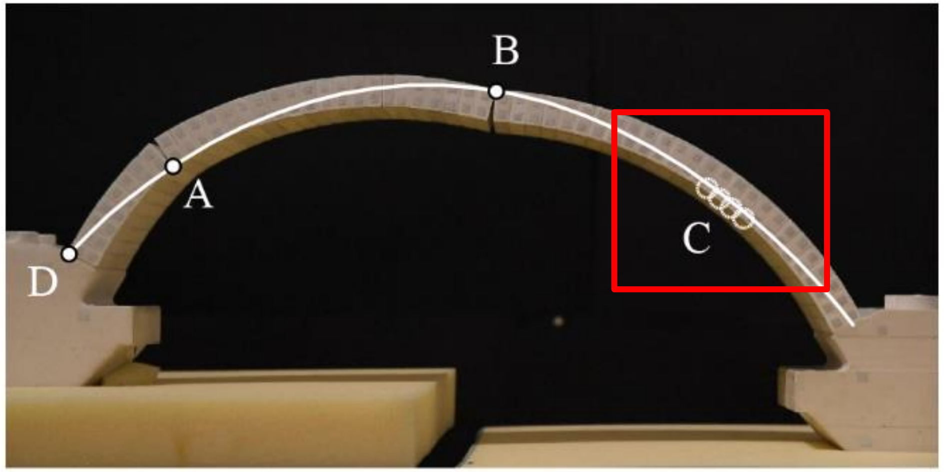

α = 20°-30°

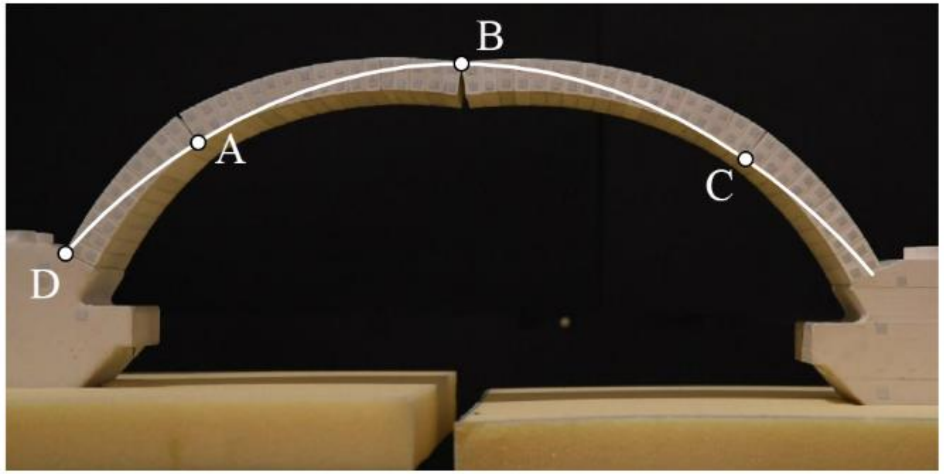

α = 35°-75°

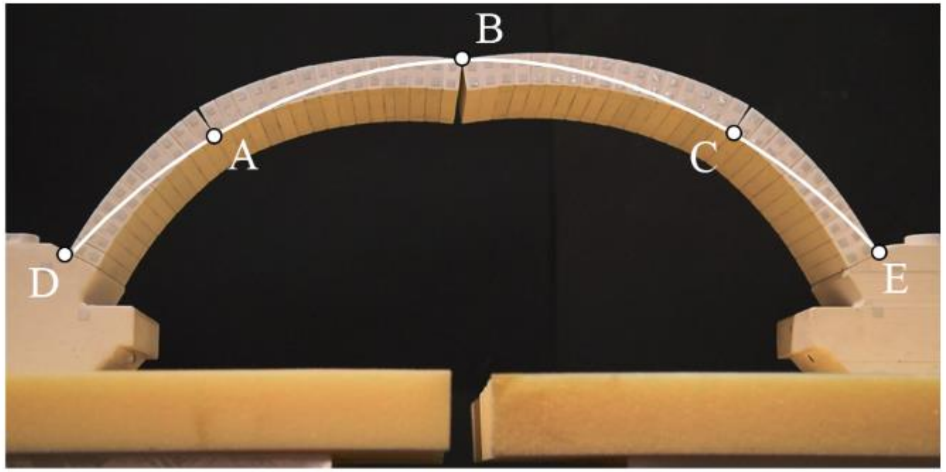

α = 90°

NUMERICAL SIMULATIONS

- Nonlinear static analyses (geometrical nonlinearities)
- **FE micro-modelling** (commercial software Diana FEA)

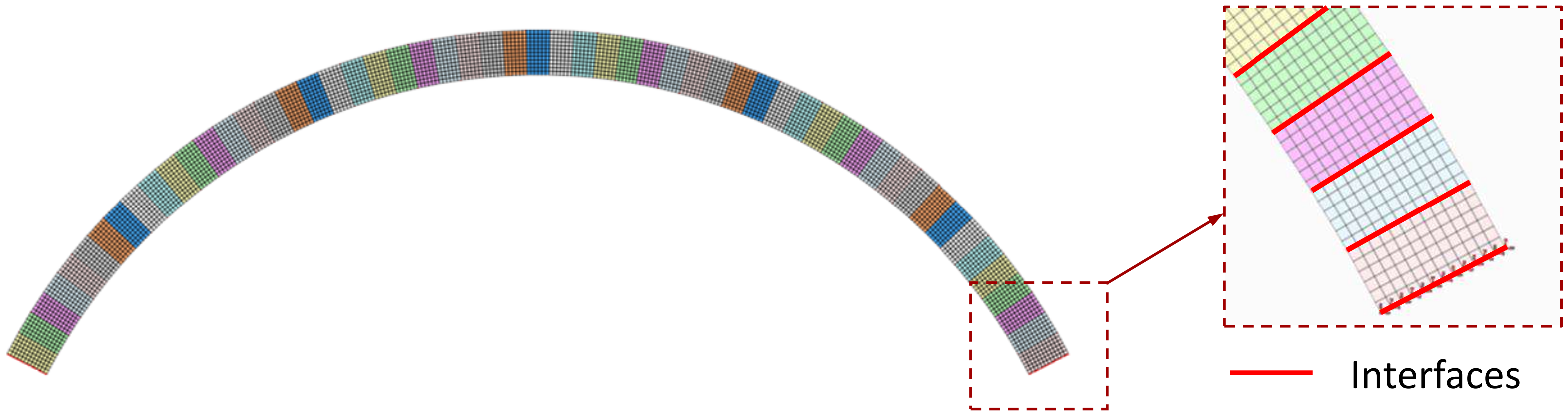

- **Linear elasticity** for the voussoirs
- **Coulomb friction model** with zero tensile strength for the interfaces
- ρ, *E* and μ taken equal to the values measured experimentally

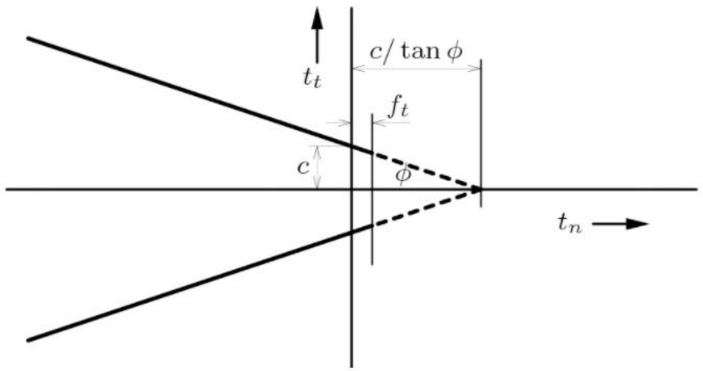

NUMERICAL SIMULATIONS

- **Sensitivity analysis to the interface stiffness for α = 0°**
  - k_n varied between 1 and 100 N/mm^3
  - k_s set equal to $0.5k_n$

NUMERICAL SIMULATIONS

- **Sensitivity analysis to the interface stiffness for α = 0°**
  - k_n varied between 1 and 100 N/mm^3
  - k_s set equal to $0.5k_n$

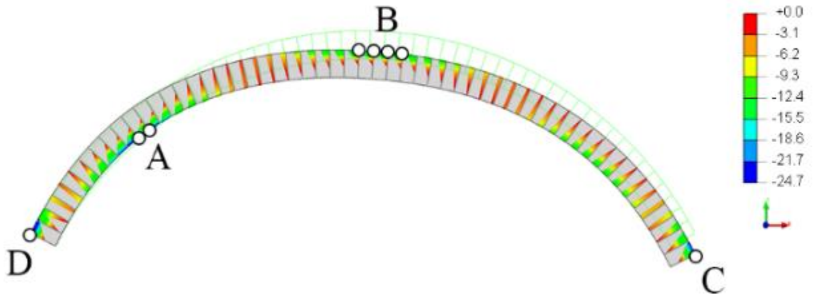

k_n = 0.1 N/mm^3

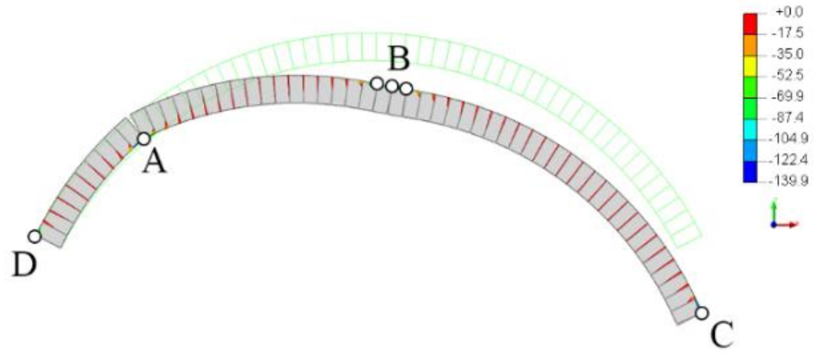

k_n = 1 N/mm^3

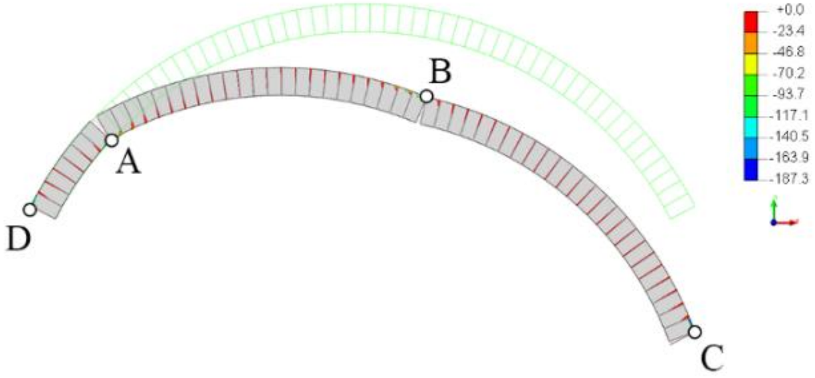

k_n = 10 N/mm^3

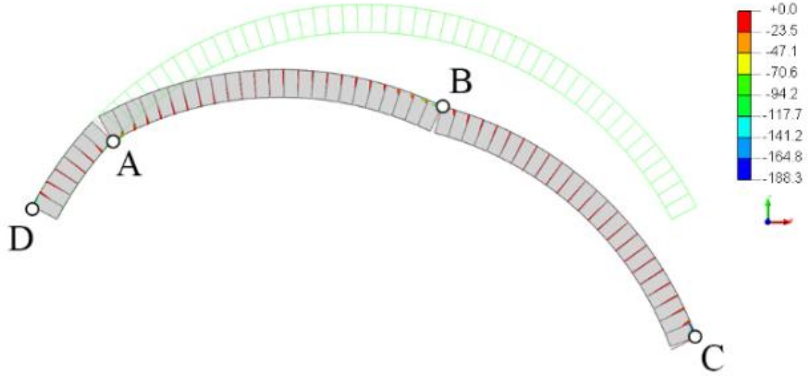

k_n = 100 N/mm^3

Collapse mechanism vs k_n

NUMERICAL SIMULATIONS

- **Sensitivity analysis to the interface stiffness for α = 0°**

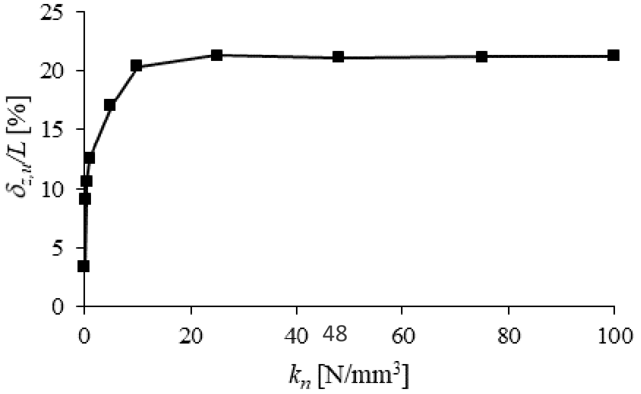

Collapse displacement
$\delta_{z,u}/L$ vs k_n

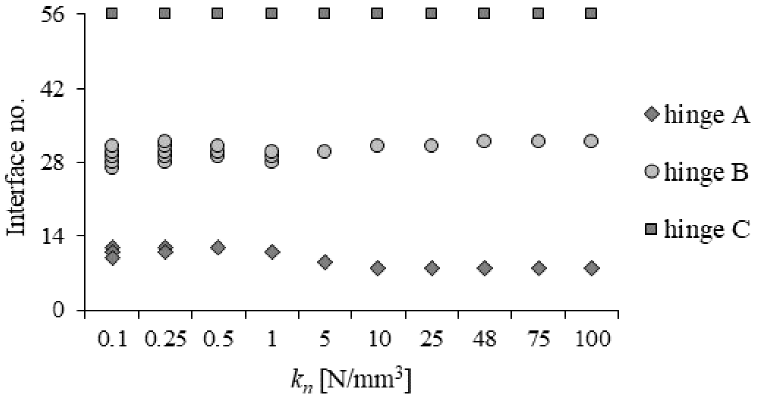

Hinge position at
collapse vs k_n

NUMERICAL SIMULATIONS

- **Sensitivity analysis to the interface stiffness for α = 0°**

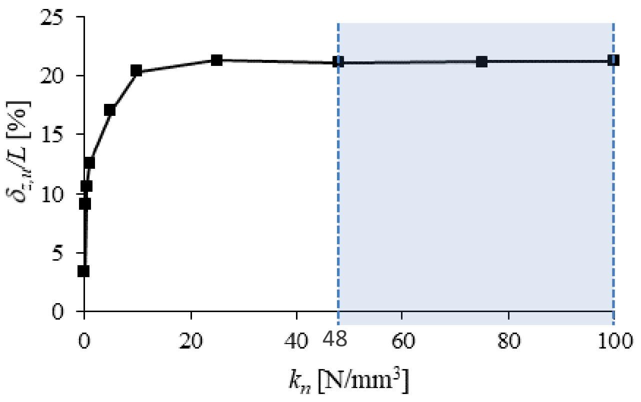

Collapse displacement
$\delta_{z,u}/L$ vs k_n

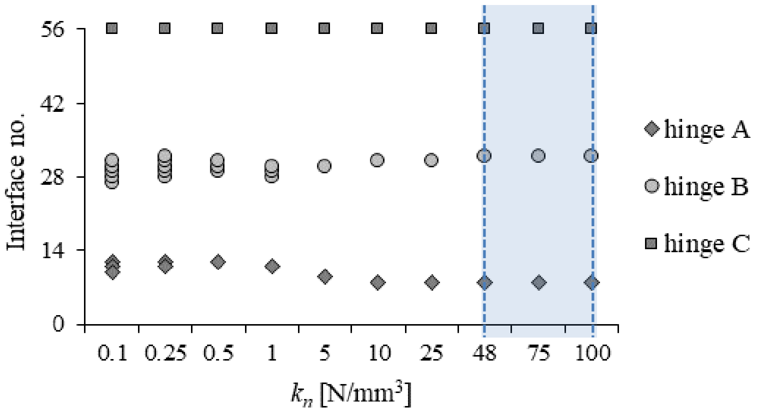

Hinge position at
collapse vs k_n

NUMERICAL SIMULATIONS

- **Sensitivity analysis to the interface stiffness for α = 0°**

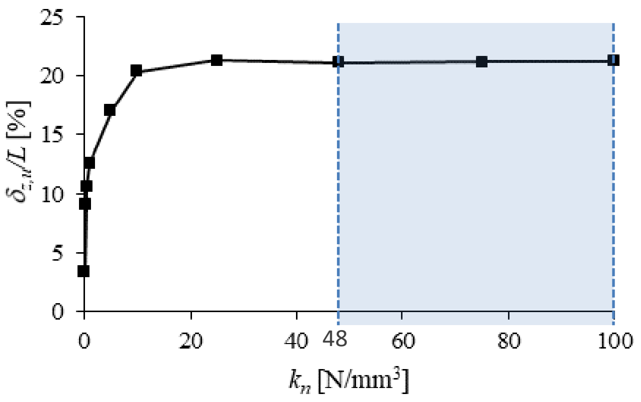

Collapse displacement
$\delta_{z,u}/L$ vs k_n

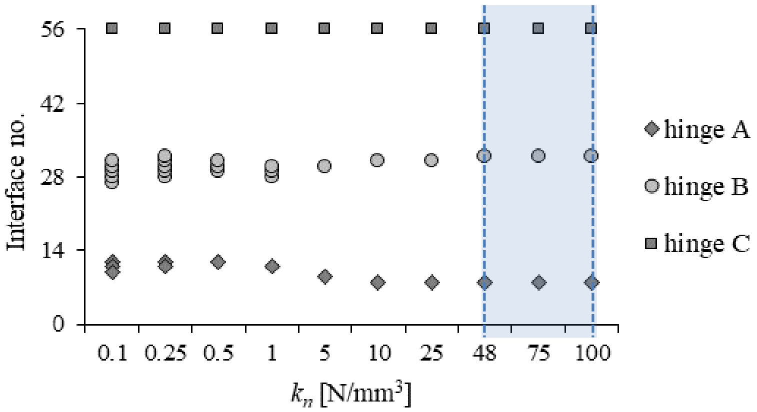

Hinge position at
collapse vs k_n

Rigid no-tension arch for
k_n = 48÷100 N/mm^3

NUMERICAL SIMULATIONS

- **Sensitivity analysis to the interface stiffness for *α* = 0°**

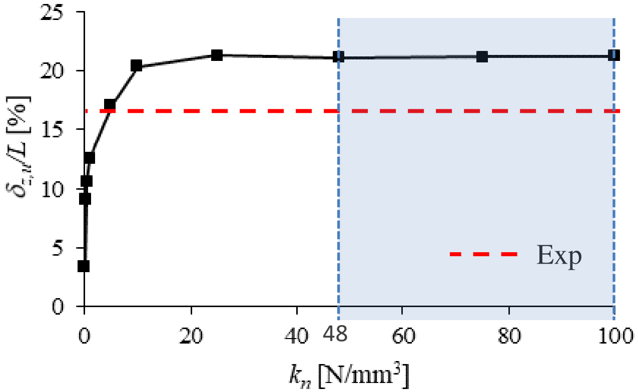

Collapse displacement
$\delta_{z,u}/L$ vs k_n

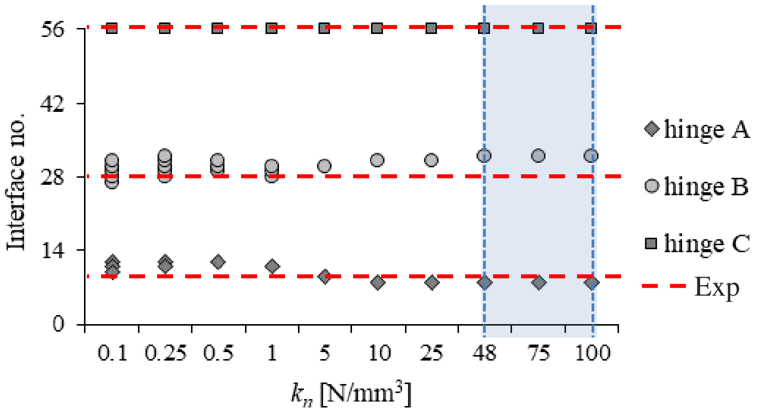

Hinge position at
collapse vs k_n

NUMERICAL SIMULATIONS

- **Sensitivity analysis to the interface stiffness for α = 0°**

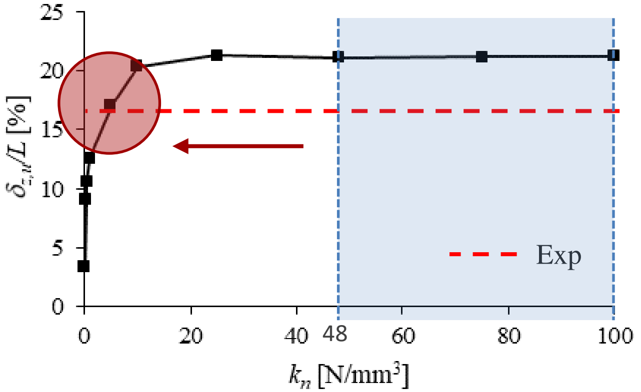

Collapse displacement
$\delta_{z,u}/L$ vs k_n

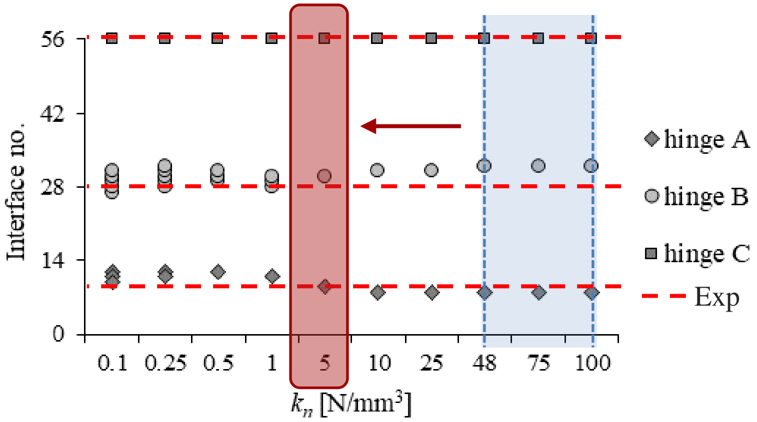

Hinge position at
collapse vs k_n

k_n should be decreased to better simulate the experimental results

NUMERICAL SIMULATIONS

- **Sensitivity analysis to the interface stiffness for α = 0°**

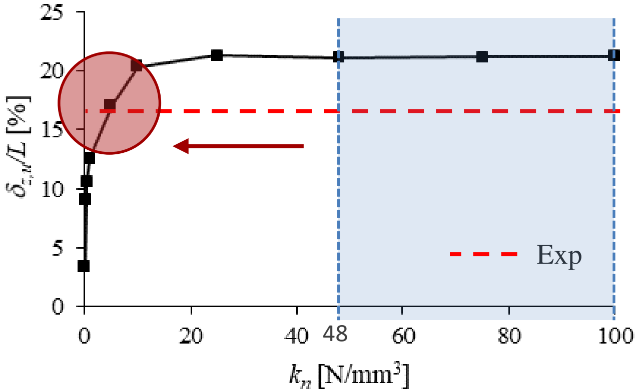

Collapse displacement
$\delta_{z,u}/L$ vs k_n

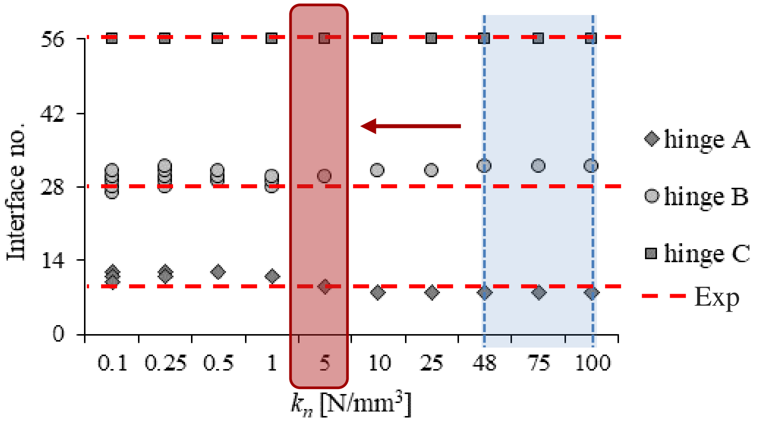

Hinge position at
collapse vs k_n

k_n should be decreased to better simulate the experimental results

The contact surfaces of the physical model **are not rigid**

JOINT DEFORMABILITY

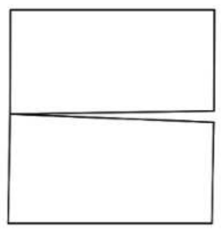

Not perfect coplanarity

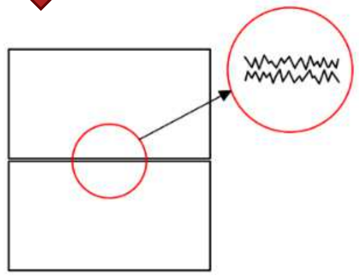

Roughness

NUMERICAL SIMULATIONS

- **Sensitivity analysis to the interface stiffness for α = 0°**

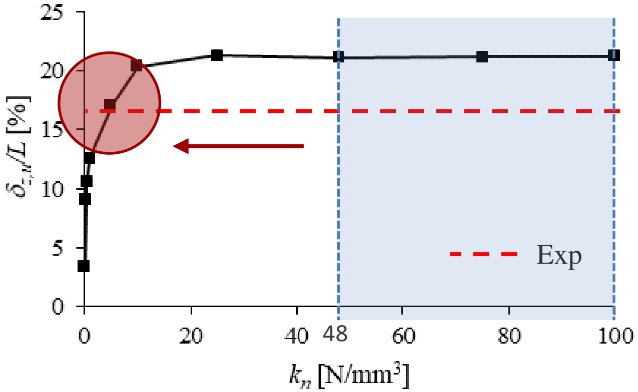

Collapse displacement
$\delta_{z,u}/L$ vs k_n

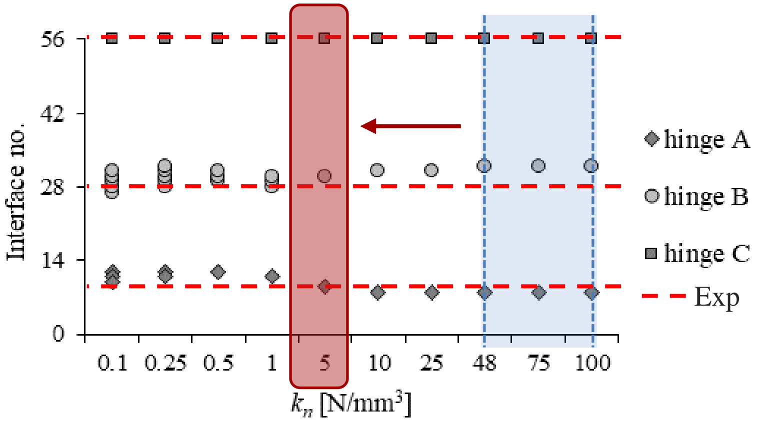

Hinge position at collapse vs k_n

k_n should be decreased to better simulate the experimental results

The contact surfaces of the physical model **are not rigid**

JOINT DEFORMABILITY

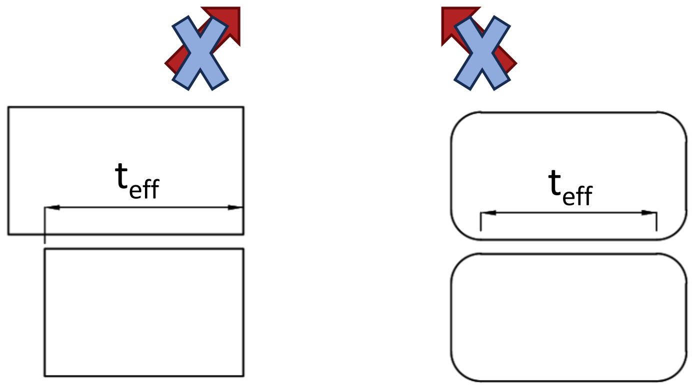

Variations in the block dimension

Corner rounding

NUMERICAL VS. EXPERIMENTAL RESULTS

- **Rigid (k_n = 48 N/mm^3) vs deformable interfaces (k_n = 3 N/mm^3) for α = 0°÷90°**

NUMERICAL VS. EXPERIMENTAL RESULTS

- **Rigid (k_n = 48 N/mm³) vs deformable interfaces (k_n = 3 N/mm³) for α = 0°÷90°**

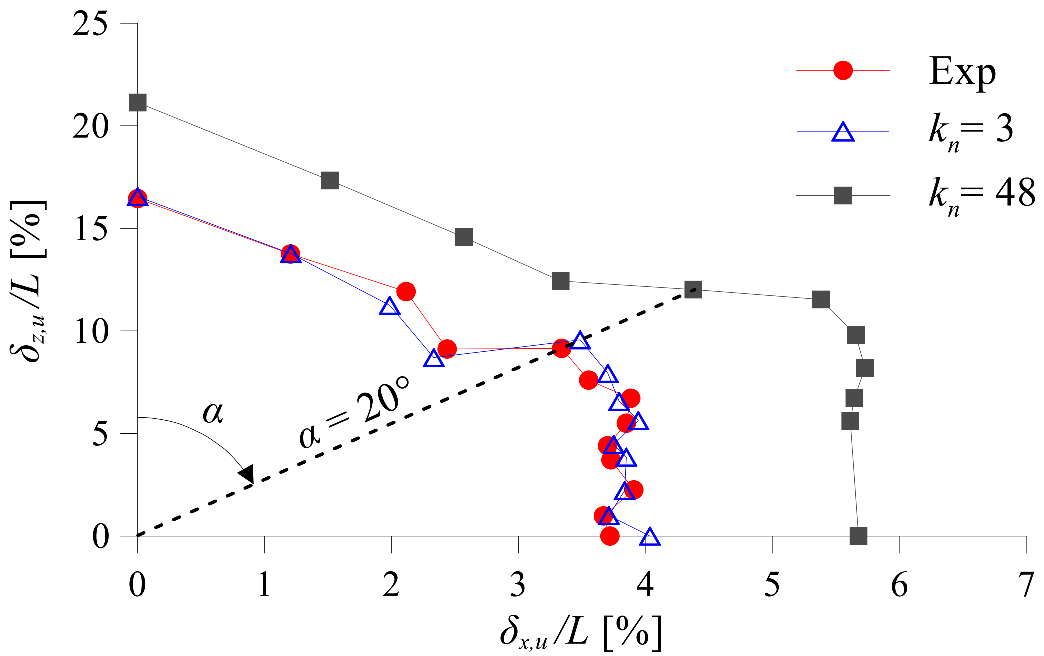

Limit displacement domain

NUMERICAL VS. EXPERIMENTAL RESULTS

- **Rigid (k_n = 48 N/mm^3) vs deformable interfaces (k_n = 3 N/mm^3) for α = 0°**

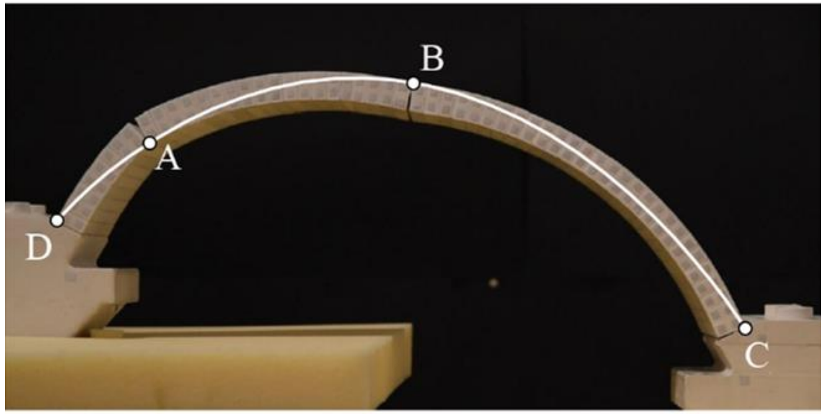

$\delta_{z,u}/L$ = 16.5 %

k_n = 48 N/mm^3

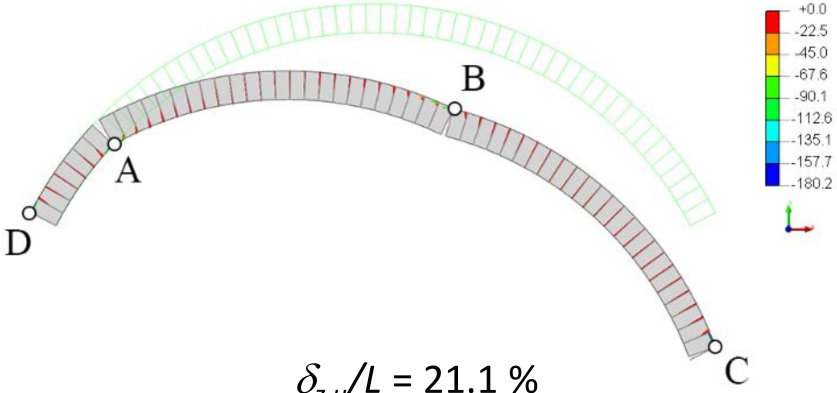

$\delta_{z,u}/L$ = 21.1 %

k_n = 3 N/mm^3

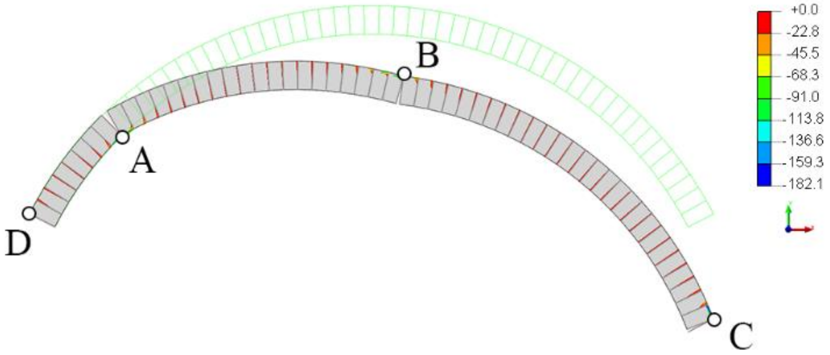

$\delta_{z,u}/L$ = 16.5 %

NUMERICAL VS. EXPERIMENTAL RESULTS

- **Rigid (k_n = 48 N/mm^3) vs deformable interfaces (k_n = 3 N/mm^3) for α = 20°**

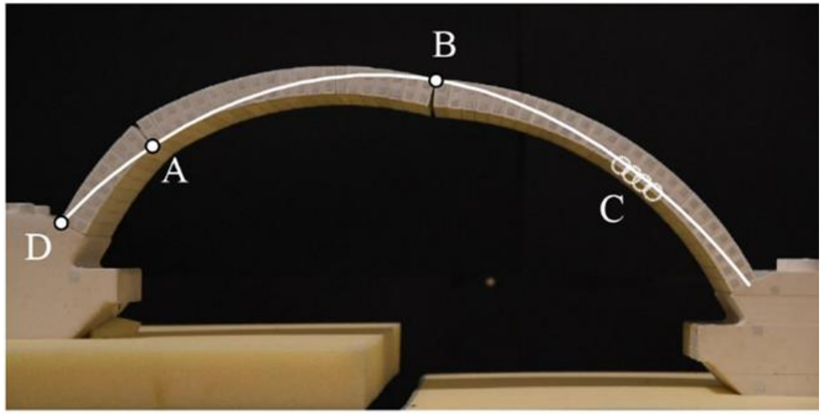

$\delta_{z,u}/L$ = 9.1 %

k_n = 48 N/mm^3

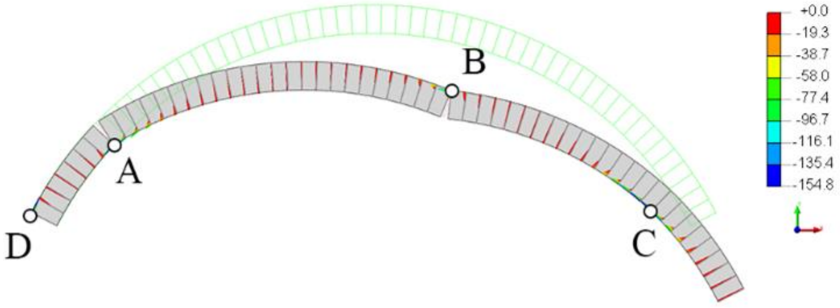

$\delta_{z,u}/L$ = 12.0 %

k_n = 3 N/mm^3

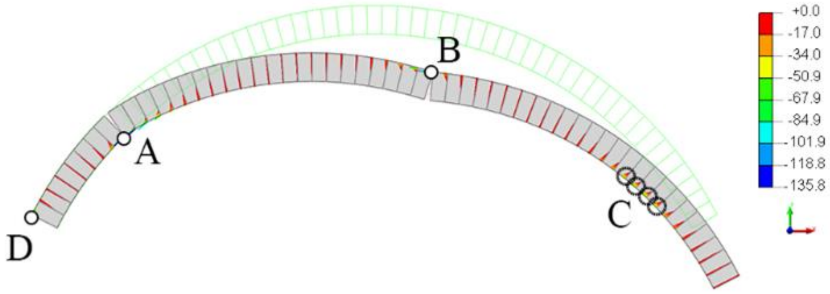

$\delta_{z,u}/L$ = 9.6 %

NUMERICAL VS. EXPERIMENTAL RESULTS

- **Rigid (k_n = 48 N/mm^3) vs deformable interfaces (k_n = 3 N/mm^3) for α = 20°**

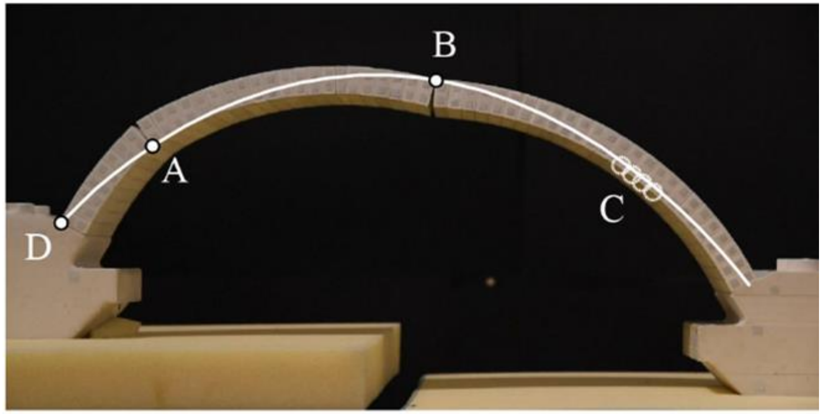

$\delta_{z,u}/L$ = 9.1 %

k_n = 48 N/mm^3

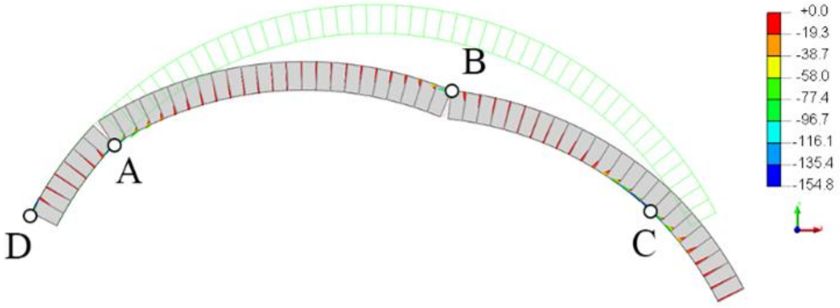

$\delta_{z,u}/L$ = 12.0 %

k_n = 3 N/mm^3

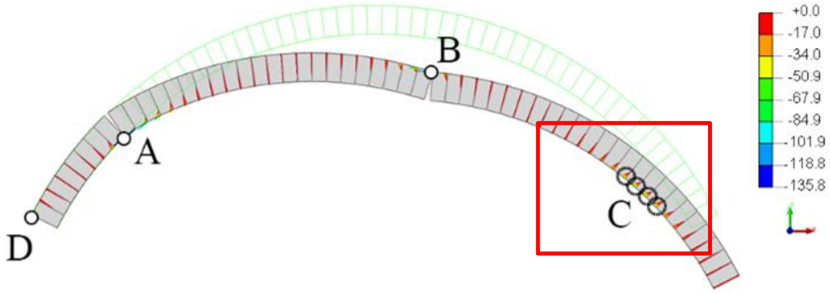

$\delta_{z,u}/L$ = 9.6 %

NUMERICAL VS. EXPERIMENTAL RESULTS

- **Rigid (k_n = 48 N/mm^3) vs deformable interfaces (k_n = 3 N/mm^3) for α = 20°**

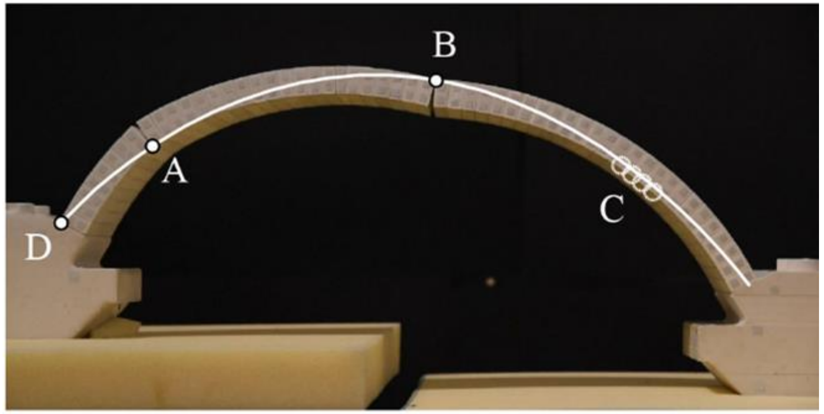

$\delta_{z,u}/L$ = 9.1 %

k_n = 48 N/mm^3

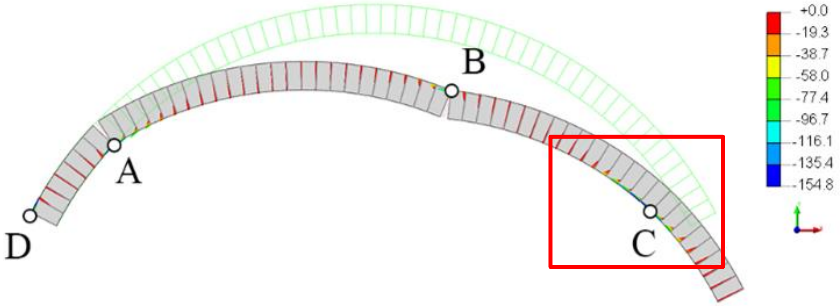

$\delta_{z,u}/L$ = 12.0 %

k_n = 3 N/mm^3

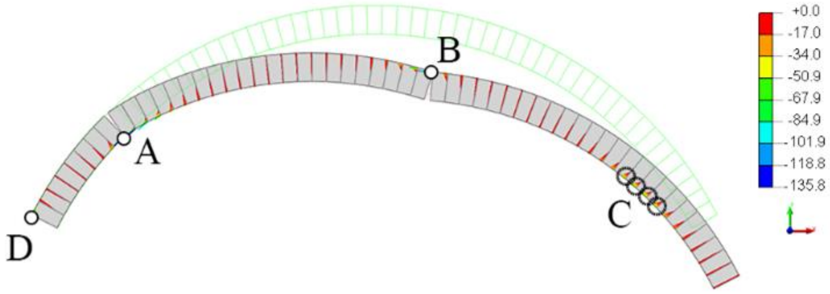

$\delta_{z,u}/L$ = 9.6 %

NUMERICAL VS. EXPERIMENTAL RESULTS

- **Rigid (k_n = 48 N/mm^3) vs deformable interfaces (k_n = 3 N/mm^3) for α = 20°**

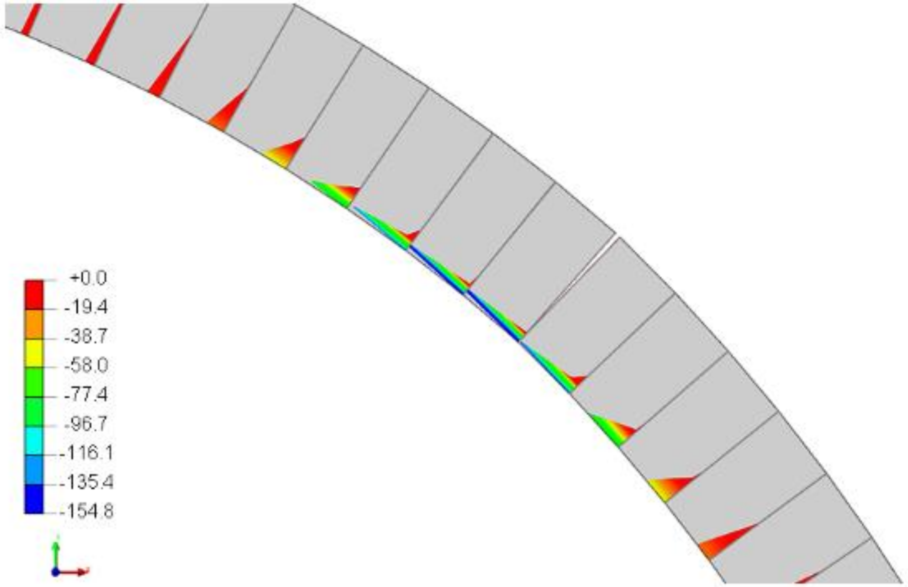

k_n = 48 N/mm^3

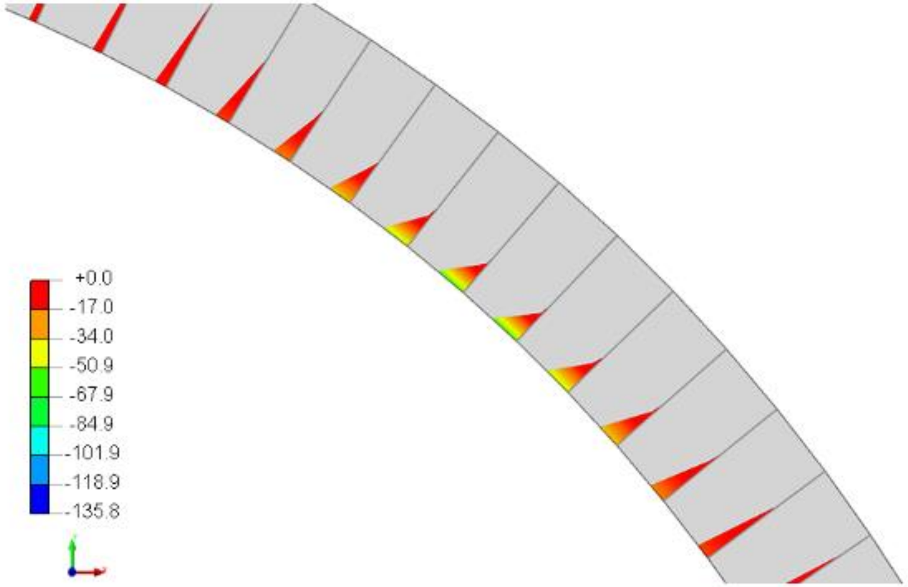

k_n = 3 N/mm^3

CONCLUSIONS

- **The direction of imposed displacements significantly influences the response** of masonry arches in terms of collapse mechanism, evolution of the hinge configuration and ultimate displacement capacity.
- Dry-joint masonry arches may not behave as rigid-no tension structures due to the **imperfections and deformability of the joints**.
- **The deformability of the joints significantly affects the collapse displacement and hinge position at collapse**, while it has little influence on the collapse mechanisms. This explains why rigid no-tension models are able to capture the actual collapse mechanisms, but they overestimate the ultimate displacement capacity.
- Joint imperfections and deformability can be included in the numerical models by **reducing the interface normal stiffness** with respect to the value adopted to simulate rigid interfaces.
- **Calibrating the interface normal stiffness** based on the experimental results is an effective strategy to accurately simulate the experimental response.

FUTURE WORK

- In-depth investigation on the effect of joint deformability and imperfections by analyzing:
  - ✓ arches with **different geometries, shapes and materials**
  - ✓ arches subjected to different **types of loading** (e.g., horizontal actions and points loads)
  - ✓ arches with **mortar joints**
  - ✓ **full-scale arches**

- Definition of **damage states** for the safety assessment of masonry arches subjected to large support displacements

ACKNOWLEDGEMENTS

Prof. Pere Roca
Department of Civil and Environmental Engineering
Polytechnic University of Catalonia (UPC), Barcelona, Spain

Prof. Chiara Calderini
Department of Civil, Chemical and Environmental Engineering
Polytechnic School, University of Genoa, Italy

THANK YOU FOR YOUR ATTENTION

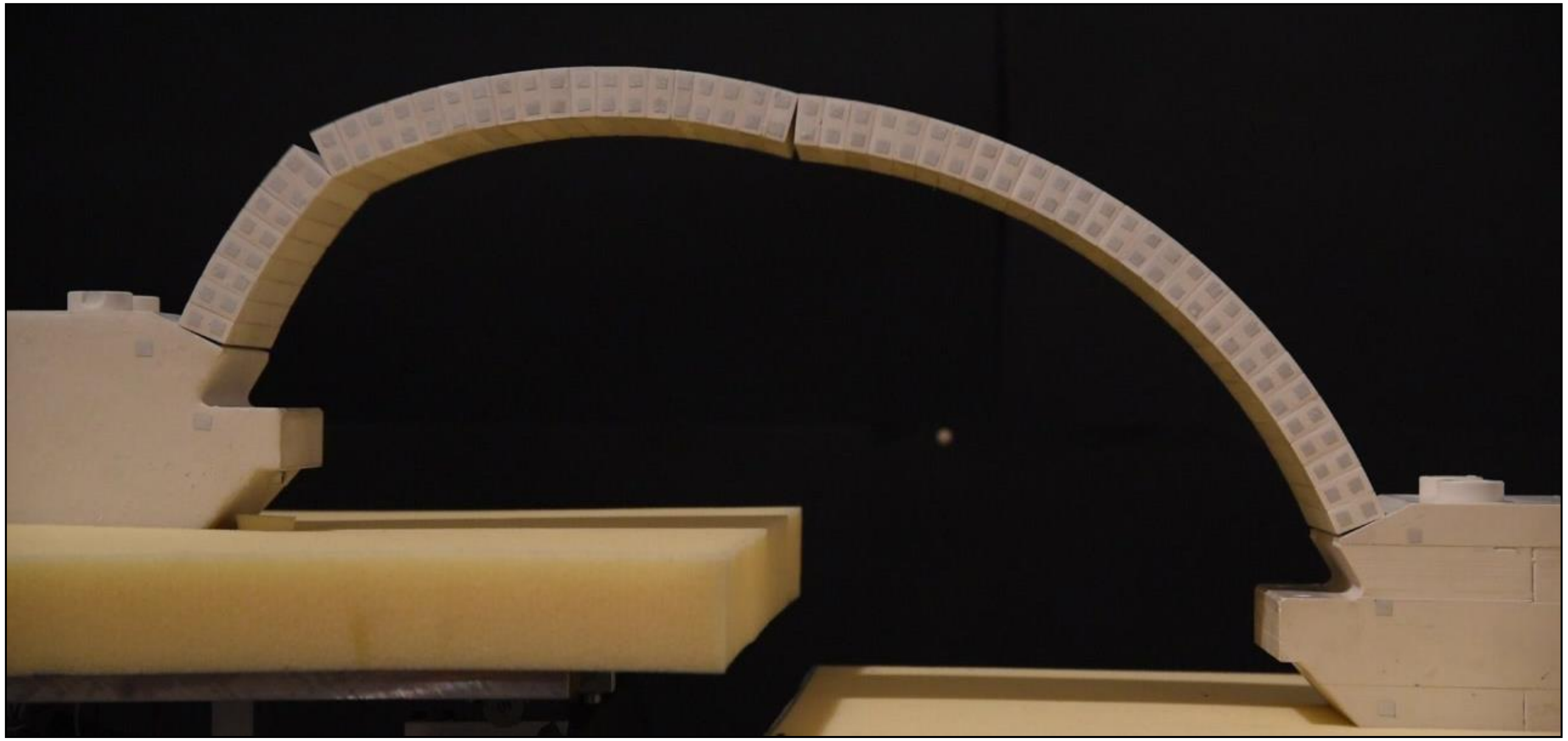

Chiara Ferrero, PhD
chiara.ferrero@edu.unige.it
Department of Civil, Chemical and Environmental Engineering
University of Genoa, Italy